Full title: The nuclear RNAi factor, NRDE2, prevents the accumulation of DNA damage during mitosis in stressful growth conditions

Short Title: Heterochromatin associated proteins and DNA damage in mitosis

Aarati Asundi[1, 2], Srivats Venkataramanan[1], Gina Caldas Cuellar[3], Atsushi Suzuki[4], Stephen N. Floor[1], Andrei Goga[1, 5, 6], Noelle L'Etoile[1]

1. Department of Cell and Tissue Biology, University of California, San Francisco, CA, USA
2. Biomedical Sciences Graduate Program, University of California, San Francisco, CA, USA.
3. Department of Molecular and Cell Biology, University of California, Berkeley, CA, United States.
4. Department of Oncology, Astellas, 2-5-1, Nihonbashi-Honcho, Chuo-ku, Tokyo 103-8411, Japan
5. Department of Medicine, University of California, San Francisco, CA, USA.
6. Helen Diller Family Comprehensive Cancer Center, University of California, San Francisco, CA, USA.

Abbreviations

PGC: Proliferative Germ Cell

NRDE-2: Nuclear RNAi Defective-2

AuBK: Aurora B Kinase

Mrt: Mortal germ line

Abstract

Organisms have evolved multiple mechanisms to prevent and repair DNA damage to protect the integrity of the genome, particularly under stressful conditions. Unrepaired DNA damage leads to genomic instability, aneuploidy, and an increased risk for cancer. Before the cell can divide, it must repair damaged DNA and it is thought that this process requires global silencing of most transcription. In *C. elegans*, NRDE-2, in complex with other nuclear factors and guided by small RNA, directs heterochromatin formation and transcriptional silencing of targeted genes. Additionally, when *C. elegans* are cultivated at high temperatures, NRDE-2 is required to maintain germ line immortality. However, the role of NRDE-2 in maintaining the physical integrity of the genome is not understood. We show here that loss of NRDE2 in either nematode or human cells induces the accumulation of DNA damage specifically under conditions of stress, such as cultivation at a high temperature in *C. elegans* or Aurora B Kinase oncogenic overexpression in the MCF10A epithelial breast cell line. In addition, we found that NRDE2 interacts with β-actin in unstressed mammalian cells. This interaction is dramatically reduced upon DNA damage. Monomeric nuclear actin binds to

heterochromatin remodeling factors and transcriptional activators while filamentous actin has been implicated in DNA repair processes. Thus, NRDE2 may dissociate from actin when it becomes filamentous as a result of DNA damage. In this way, heterochromatin factors may associate with the actin dependent DNA repair process to allow appropriate mitotic progression and maintain genomic integrity.

Introduction

Organisms have developed multiple ways to protect genomic integrity during mitotic cell division. Maintenance of the physical and informational integrity of the genome ensures that cells accurately transmit genetic information from one generation to the next, thereby safeguarding against diseases associated with genomic instability, such as cancer. Genomic instability is caused primarily through DNA damage. DNA damage can be incurred in a number of ways, including naturally during DNA replication, meiotic recombination, improper chromosome segregation, and transposable elements. DNA damage can also be caused by external sources such as UV irradiation or drugs. If the cell attempts to divide before the DNA is repaired, the unrepaired DNA damage can result in mitotic delay, aneuploidy, or apoptosis, which in turn can lead to disorders in the organism including cancer and infertility.

To protect against genomic instability, cells must fulfill a checkpoint at the Gap2 to Mitosis (G2/M) transition [46] at which the cell repairs any DNA damage sustained during the previous cell cycle phases. If the requirements of the G2/M checkpoint are

not satisfied, the cell will express a number of cell cycle inhibitors, leading to an arrest in G2. [30]

DNA repair is especially important in the germ line where strong evolutionary pressure to maintain the integrity of the genome of germ cells selects against harmful mutations. Thus, the germ line provides a window into how the environment affects the cell cycle. The nematode *Caenorhabditis elegans* has a well-characterized germ line and reproductive cycle, which can be used to study the effects of improper mitosis on cell fate and fertility. The adult *C. elegans* gonad contains a stem cell niche, which mitotically proliferates to self-renew. These proliferating germ cells (PGCs) constitute the only pool of mitotically dividing cells in the adult worm. As the PGCs divide, they travel proximally along the gonad, where they transition from mitotic proliferation to meiotic division and ultimately differentiate into spermatozoa or oocytes. Therefore, maintaining mitotic integrity in the PGC pool is essential for ensuring the reproductive integrity of the animal.

Previous studies show that the number of PGCs is susceptible to internal molecular changes as well as external stresses, which can impact the worm's fertility. In addition to canonical signaling, such as the GLP-1/Notch, [31-32] DAF-7/TGFb [33] and IGF-1/insulin [34] pathways, many small RNA pathway proteins have also been extensively studied in the context of maintaining the PGC pool and fertility. For example, mutations in CSR-1 (argonaute that binds endogenous 22G siRNAs)[36], EGO-1 (putative RdRP required for small RNA biosynthesis) [37, 38], DCR-1 (cleaves dsRNA) [39, 40] and EKL-1 (Tudor domain protein required in 22G RNA biosynthesis) [36, 41] have all been shown to have

significant mitotic and meiotic germ cell defects. Furthermore, external stresses such as starvation or changes in cultivation temperature can directly impact the PGC pool and subsequently affect fertility. [34, 35]

In particular, the nuclear RNAi protein, NRDE-2 is required to maintain reproductive integrity of *C. elegans* in response to environmental stress. *Nrde-2* null mutants remain fertile indefinitely at when grown under normal conditions at 20°C, however, when propagated at 25°C they produce fewer progeny each successive generation until becoming completely sterile by the fourth generation. [1, 16] This progressive sterility is termed a mortal germ line phenotype (Mrt). *Nrde-2* null mutant worms grown at 25°C also express high levels of repetitive RNA as compared to wild type worms propagated under the same conditions. This is consistent with the hypothesis that NRDE-2 acts to silence transposons and repress repetitive sequences, [16, 47] which are naturally occurring DNA damaging agents and can affect the informational and physical integrity of the genome.

We and others have hypothesized that the Mrt phenotype seen in *C. elegans* mutants lacking heterochromatin factors, piRNA, or nuclear RNAi factors, including NRDE-2, might result from accumulated DNA damage in the germ line. [47] The function of NRDE-2 in preventing DNA damage accumulation seems to be conserved across species but had not been directly studied in the *C. elegans* germ line. In the fission yeast, *S. pombe*, loss of the NRDE-2 homolog (known as nrl1) results in increased DNA damage, which was posited to arise from unresolved R-loops. [17] R-loops are RNA-DNA hybrids that arise from transcription of repetitive elements in which the RNA message invades

the double stranded DNA helix. The DNA-RNA hybrid is more stable than the DNA-DNA hybrid and can cause DNA damage when the replication fork collides with it. Transcriptional silencing of repetitive elements by heterochromatin factors such as NRDE2 was thought to prevent the possibility of R-loop formation. [48] A recent study in HEK293 (human embryonic kidney) cells, however, showed the human homolog of NRDE-2 (known as NRDE2 or C14orf102) plays a role in DNA damage response and preventing the accumulation of double stranded breaks, independently of R-loop formation and resolution. [22] Thus, NRDE2 may act in its capacity as a heterochromatin factor to repress transcription of repetitive elements to limit both R-loop formation and transposition, which are two events that pose threats to the integrity of the genome. Recently, it has been increasingly appreciated that heterochromatic regions of the genome (nuclear speckles) are associated with monomeric actin and that heterochromatin remodelers such as SWI/SNF , SWR1 and INO80 are tightly bound to actin monomers and this association is important for their ability to bind to chromatin. [45] Thus, stressors such as high temperature and DNA damage have been shown to tilt the balance of nuclear actin from monomeric to filamentous, which has been shown to be required for efficient DNA damage repair. [25] How heterochromatin associated factors and nuclear actin polymerization status are linked, however, remains unclear. In this paper, we show evidence that NRDE2 prevents the accumulation of DNA damage particularly under conditions of stress in proliferating cell populations. In the *C. elegans* germ line, NRDE-2 loss resulted in the accumulation of DNA damage only when the worms were propagated at a high temperature. This correlated with a decrease in the

number of PGCs and was consistent with the previously reported Mrt phenotype. Moreover, in human cells, we found that NRDE2 loss did not significantly impact the proliferation of normal epithelial breast cells MCF10A unless they overexpress the oncogene Aurora B Kinase (AuBK). In these cells, we observed a delay in mitotic prophase as well as an increase in DNA damage. This indicates that NRDE2 may have a role protecting against DNA damage accumulation. Finally, we observed a strong protein-protein interaction between NRDE2 and β-actin in normally proliferating MCF10A cells, which was weakened upon the introduction of DNA damaging agents. Thus, we suggest a novel link between this heterochromatin factor, actin, and DNA repair.

Results

Loss of NRDE-2 coupled with propagation at high temperature incurs DNA damage in the mitotic zone of the C. elegans gonad

Previous studies in *C. elegans* have shown that loss of NRDE-2 does not affect germ line immortality when the worms are propagated at 20°C. We have observed that although *nrde-2 (gg91),* null mutants remain fertile indefinitely when cultivated at 20°C, these worms have a lower brood size as compared to wild type (Fig S1, p=0.0148, n=4). In contrast, if the worms are cultivated at 25°C, a more stressful temperature, *nrde-2 (gg91)* mutants exhibit a Mrt phenotype that increases in severity with each successive generation.[1] We asked whether the decrease in brood size of *nrde-2 (gg91)* mutant worms was a result of physiological defects in the gonad. We observed a significant

132 decrease in the number of proliferating germ cells (PGCs) in the mitotic zone in *nrde-2*
133 *(gg91)* worms propagated at 20°C as compared to wild type (Fig 1A and B, left,
134 p=0.0115). When we propagated the worms at the stressful temperature of 25°C for 2
135 generations (G2), we found that the number of PGCs was significantly decreased as
136 compared to wild type G2 worms grown at 25°C (Fig 1A and B, left, p<0.0001).
137 Since the Mrt phenotype in *nrde-2 (gg91)* mutants depends on cultivation at 25°C, we
138 asked whether the cells accumulated DNA damage at this temperature, which would
139 ultimately cause sterility. We used immunofluorescence to stain for RAD-51, a marker of
140 DNA damage repair, and found that *nrde-2 (gg91)* G2 worms grown at 25°C had
141 significantly increased RAD-51 foci in the mitotic zone as compared to wild type G2
142 worms grown at the same temperature (Fig 1A and B, right, p<0.0001). We then asked
143 whether the aberrant accumulation of DNA damage in the mitotic PGCs resulted in
144 defects as the cells entered meiosis in the proximal gonad and progressed towards
145 oocyte formation. We expressed the apoptotic cell corpse marker, CED-1::GFP, which
146 labels apoptotic cell corpses in the proximal loop of the gonad, in *nrde-2 (gg91)* mutants
147 and wild type worms. We found that when the worms were propagated at 20°C, *nrde-2*
148 *(gg91)* mutants showed a similar number of CED-1::GFP labeled germ cell corpses as
149 wild type worms. However, *nrde-2 (gg91)* G1 and G2 worms showed increased numbers
150 of CED-1::GFP labeled germ cell corpses as compared to wild type G1 and G2 worms,
151 respectively (Figure 1C and D, p<0.0001 for both).
152 We conclude that when worms are cultivated at a normal, non-stressful temperature,
153 loss of NRDE-2 has minor endurable impacts on fertility and integrity of the *C. elegans*

154 germ line. However, when NRDE-2 loss is coupled with an external stress, such as a high
155 cultivation temperature, the DNA damage and subsequent cell death in the gonad
156 compounds over the generations, ultimately resulting in sterility. Therefore, we
157 propose the NRDE-2 may have a role in preventing DNA damage accumulation in the
158 mitotic PGCs in order to maintain integrity of the *C. elegans* germ line.
159
160 Loss of NRDE2 coupled with Aurora B Kinase overexpression in MCF10A cells results in
161 DNA damage accumulation
162 To gain a biochemical and cell biological understanding of the role of NRDE-2, we
163 decided to utilize the actively dividing MCF10A cell line. MCF10A cell are a normal
164 human epithelial cell line derived from reduction mammoplasty. [4]
165 We used a lentiviral vector to stably express an eGFP-tagged version of human NRDE2 in
166 the MCF10A cells. The eGFP::NRDE2 localized to puncta within the nucleus (Fig 2Ai).
167 These puncta were reminiscent of staining of heterochromatin and heterochromatin
168 associated factors. [49] Once the cell entered prophase, as characterized by chromatin
169 condensation, the eGFP signal became diffuse and remained so throughout mitosis (Fig
170 2Aii-v) until cytokinesis, when eGFP::NRDE2 seemed to re-localize to puncta in the
171 nuclei of the daughter cells (Fig 2Avi). The dynamics of this pattern of staining is similar
172 to that of human RNA pol II transcription machinery proteins TBP (TATA box-binding
173 protein) and TAF12 (TATA box-binding protein associated factor 12) in HeLa cells. [29]
174 These data are therefore consistent with a conserved role for NRDE2 as a transcriptional
175 regulator in human cells.

We wanted to further test the hypothesis that NRDE-2 regulates DNA damage and mitosis under stressful conditions. We therefore created a mitotically stressed MCF10A cell line by stably overexpressing an HA-tagged version of the oncogene Aurora B kinase (AuBK OE) in eGFP::NRDE-2 expressing cells. AuBK is a master regulator of mitotic events, including chromatin condensation during prophase, [5] microtubule-kinetochore attachment during metaphase, [6], [7] and abscission during cytokinesis. [8] Loss of this regulation has been linked to genetic instability, which results in aneuploidy, a key hallmark of cancer. Accordingly, AuBK over-expression has been linked to many cancer types and correlates with poor prognosis for patients. [11-12] The localization of eGFP::NRDE2 in AuBK OE MCF10A cell lines throughout the cell cycle was identical to that of eGFP::NRDE2 in control cells (Fig 2A vii and xii).

Consistent with AuBK's role in mediating chromatin condensation at the G2/M transition, AuBK OE MCF10A cells showed increased levels of phosphorylated Histone H3 (Fig 2B, middle, $p=0.0337$, $n=4$), a known target of Aurora B Kinase. We also observed a significant increase in γH2AX (H2AX phosphorylation on S139), a common marker of DNA damage (Fig 2B, right, $p=0.015$, $n=5$). Therefore, we utilized AuBK overexpression as a tool to study the effects of NRDE2 loss on DNA damaged cells.

Next, we assessed the efficacy of using NRDE2 targeted siRNA as a tool to knockdown NRDE2 in MCF10A cells. We observed that cells treated with NRDE2 siRNA showed >90% decrease in eGFP::NRDE2 expression as compared to cells treated with a non-targeting siRNA control (Fig 2C). We then asked whether the amount of DNA damage in control or AuBK OE cells was altered upon NRDE2 knockdown. Interestingly, we found when

198 control cells were treated with NRDE2 siRNA, there was no increase in γH2AX as
199 compared to control cells treated with non-targeting siRNA (Fig S3, p=0.11, n=5).
200 However, loss of NRDE2 in AuBK OE cells resulted in increased DNA damage as
201 compared to AuBK OE cells treated with non-targeting siRNA (Fig 2D, p=0.048, n=5). We
202 conclude that loss of NRDE2 has a minimal effect on DNA damage in normally
203 proliferating cells. However, in AuBK OE cells, which show an increased basal level of
204 DNA damage, loss of NRDE2 further increases the accumulation of DNA damage.
205
206 *Loss of NRDE2 coupled with Aurora B Kinase overexpression in MCF10A cells results in*
207 *mitotic delay*
208 We asked whether the increase in DNA damage observed in the AuBK OE cells upon
209 NRDE2 loss would result in an observable change in mitotic cell proliferation. We
210 observed that when AUBK OE cells were treated with NRDE2 siRNA, there was a
211 decrease in overall metabolic cell activity in the culture (Fig S2) and a significant increase
212 in the number of rounded cells (Fig 3A). Cells commonly round up due to a stall in
213 mitosis or when the cell is about to undergo apoptosis, both of which could explain the
214 observed decrease in metabolic cell activity. To differentiate between these two
215 possibilities, we used live cell imaging to record cell growth after NRDE2 knockdown. We
216 found that AuBK OE cells treated with non-targeting siRNA took a longer time to
217 complete mitosis than control cells. Furthermore, when AuBK OE cells were treated with
218 NRDE2 siRNA, there was a significant increase in the average time through mitosis (Fig
219 3B and C). However, we also noticed that a small proportion of AUBK-overexpressing

cells required a significantly longer time to complete mitosis upon NRDE2 siRNA treatment (Fig 3B and C). The rounded morphology of the cells, the compaction of the chromatin and the concentration of the DNA at the cell center, indicated that this stall may occur during the early stages of mitosis.

We propose that the rounded cells observed upon NRDE2 knockdown in AUBK-overexpressing cells is due to a delay in mitosis. To further characterize this delay, we calculated the mitotic index of these cells. Consistent with the time lapse data, we found that AuBK OE cells had a higher mitotic index than control cells. However, we found no significant difference between the mitotic index of non-targeting siRNA treated cells and the NRDE2 siRNA treated cells in either the control or AuBK OE (Fig S4). We surmised that this could be due to the fact that the percentage of cells with a significant delay in mitosis is so low that these cells were not sufficient to affect the mitotic index.

We next asked whether we could identify the stage at which mitosis was delayed in AUBK-OE cells. We quantified the number of cells in each stage of mitosis in a fixed population of cells and found more cells in prophase upon NRDE2 knock down (Fig 3E p= 0.025, n=4). This is also consistent with the time lapse analysis of AuBK OE cells delayed in early mitosis (Fig 3C) leading us to conclude that the delay seen in NRDE2 knockdown AUBK-overexpressing cells may be occurring at prophase.

Mammalian NRDE2 interacts with β-actin in healthy, normally proliferating cells, and this interaction is weakened upon DNA damage

Our finding that NRDE2 specifically mitigates DNA damage accumulation in sensitized or stressed cell populations led us to ask whether NRDE2 interacts with different partners under these conditions. We decided to probe this question using co-immunoprecipitation experiments, using an anti-GFP antibody to detect eGFP::NRDE2 in MCF10A lysates (Fig 4A and Fig S5).

In *C. elegans*, NRDE-2 interacts with other nuclear RNAi factors NRDE-1 and NRDE-4, as well as the worm specific argonaute NRDE-3. [11] In contrast, NRDE2 does not interact with other RNAi factors in S. pombe yeast cells or in human cells. [22, 43, 44] Consistent with these findings, we saw no interaction between eGFP::NRDE2 and any of the known human Argonautes AGO-1/2/3/ or -4 (Fig S6).

Interestingly, we observed a strong interaction between NRDE2 and β-actin in control cells (Fig 4A). Furthermore, this interaction seemed to be weakened in AuBK OE cells (Fig 4A and B, p=0.036, n=5). These results may suggest an interesting function for NRDE2 in DNA damaged cells. Nuclear actin forms filaments upon DNA damage to aid in repair. [25] Since AuBK overexpression increases DNA damage in MCF10A cells, we hypothesized that the interaction between NRDE2 and β-actin may be weakened in these cells due to the nuclear actin forming filaments in response to DNA damage. To test whether DNA damage altered the interaction between NRDE2 and β-actin, we treated the cells with cisplatin, a DNA damaging reagent. In both control and AuBK overexpressing MCF10A cells, the interaction between NRDE2 and β-actin was reduced as compared to untreated cells (Fig 4A and B, p=0.045, n=3). Therefore, we propose that NRDE2 interacts with β-actin only when the DNA is intact. However, when DNA damage

263 in induced by stressors such as AuBK over-expression or the presence of cisplatin, the
264 interaction between NRDE2 and β-actin is disrupted, perhaps as a result of the nuclear
265 actin forming filaments to aid in DNA repair.
266
267 **Discussion**
268 This study describes a previously uncharacterized role for NRDE2, a putative nuclear
269 RNA-binding protein, in protecting against DNA damage in stressed cells. Our study is
270 the first to study the effect of NRDE2 loss in normal, unstressed cells as compared to in
271 stressed cells. We have also shown that this protective role for NRDE2 in stressed cells is
272 conserved in *C. elegans* and mammalian mitotic cells.
273 Previously, NRDE2 was described to protect against the accumulation of DNA damage,
274 as assessed by an increase in γH2AX levels upon NRDE2 loss in HEK293 cells. [22] We
275 believe this is consistent with our results as HEK293 cells are not a normally proliferating
276 cell line. The HEK293 line was originally obtained by transforming human embryonic
277 kidney cells with human adenovirus type 5, resulting in a 4.5kb insertion of a viral
278 fragment in chromosome 19 which interferes with cell death and cell cycle control
279 pathways. [23] HEK293 cells are also hypotriploid, [24] which may further affect mitosis.
280 Consistent with this point, we found that NRDE2 knockdown resulted in an increase of
281 γH2AX levels only in AuBK-overexpressing MCF10A cells, not in the normal, unstressed
282 control cells. Since AuBK overexpressing causes an increase in basal levels of DNA
283 damage, we propose that NRDE2 in mammalian cells results in an accumulation of DNA

damage only in cells with increases mitotic stress, similar to the results seen in *C. elegans*.

In *C. elegans*, loss of NRDE-2 alone does not seem to severely compromise the mitotic PGCs or brood size, as evidenced by the worms remaining indefinitely fertile and exhibiting relatively normal development. Upon the addition of a stressful 25°C cultivation temperature, however, there is a drastic reduction in the number of PGCs and brood size. Under these stressful conditions, DNA damage accumulates in the germ cells, presumably resulting in the previously observed Mrt phenotype. This trans-generational Mrt phenotype is similar to fertility defects observed *rsd-2* and *rsd-6* RNAi spreading defective mutants. RSD-2 and RSD-6, along with NRDE-2 were proposed to induce genome wide epigenetic silencing to maintain germ cell immortality and fertility. RSD-2 and RSD-6 are also thought to act in a different pathway than the 22G-RNA associating argonautes CSR-1 and ALG3/4, which display Mrt phenotypes due to defects in spermatogenesis. [16] The effect of NRDE-2 loss on spermatogenesis remains unclear.

The defects seen in *nrde-2 (gg91)* mutants may also be due to improper chromatin condensation and chromosome segregation. It has been previously reported that CSR-1 is required for the localization of CDE-1, a nucleotidyltransfease protein that is responsible for the uridylation of siRNAs bound by CSR-1, to mitotic chromosomes in embryos. [19] Loss of CDE-1 results in an accumulation of siRNAs and improper gene silencing, as well as mitotic and meiotic chromosome segregation defects. NRDE-2, by

306 contrast, associates with other NRDE pathway proteins to recruit methlytransferases
307 MES-2 and SET-25, which direct the deposition of methylation marks to silence loci
308 targeted by siRNAs. [20-21] Therefore, NRDE-2 loss may also result in improper gene
309 silencing in the *C. elegans* germ line, resulting in mitotic defects, which are exacerbated
310 by the stress of high temperature.
311
312 Interestingly, we observed a strong association between NRDE2 and β-actin in MCF10A
313 cells that was diminished upon DNA damage causing agents. Since NRDE2 localizes to
314 puncta in the interphase nucleus, we hypothesize that NRDE2 likely interacts with
315 nuclear actin. One potential model for this interaction is that NRDE2 binds to
316 monomeric nuclear actin in the unstressed cell. Monomeric nuclear actin associates
317 with chromatin remodeling complexes, and might be involved in chromatin binding. [45]
318 However, upon DNA damage, nuclear actin assembles into filaments and promotes DNA
319 damage repair. [25] NRDE2 may be displaced or unable to bind to filamentous actin, and
320 as a result, show a weakened interaction on β-actin upon DNA damage. It is still unclear
321 whether NRDE-2 functions in preventing the formation of DNA damage or as a
322 chromatin associated sensor of DNA damage in the β-actin dependent DNA repair
323 pathway. Further study is needed to characterize the function of NRDE2, and possibly
324 other heterochromatin factors, in preventing DNA damage accumulation and
325 maintaining genomic stability. The interaction between NRDE2 and β-actin is especially
326 exciting as it may indicate a new mechanistic role for NRDE2 in the nucleus beyond gene
327 silencing and epigenetic inheritance.

Materials and Methods

C. elegans strains

All strains were cultured on Nematode Growth Medium (NGM) plates seeded with E. coli OP50. Bristol N2 was the wild type strain used. Loss of NRDE-2 was studied using the mutant allele *nrde-2 (gg91).* Worms were crossed into a strain expressing ced-1p::GFP+ lin-15 (+) to study apoptotic cells.

Gonad Staining

Gonads were dissected from young adults (24 hours post-L4 stage) in 1xEGG buffer (25mM HEPES, pH7.3; 118mM NaCl, 48mM KCl, 2mM CaCl2, 2mM MgCl2) and fixed in 2% (final concentration) formaldehyde. The following primary antibodies were used: rabbit anti-RAD-51 and chicken anti-HTP-3. Fixed gonads were imaged with exposure times of 100ms with DAPI, GFP, TRITC, and CY5 filter cubes and a mercury arc lamp on a Zeiss AxioPlan2 epifluorescence microscope (operated by MicroManager 1.4.13) with a 60x 1.3 DIC oil objective and a QIClick camera (QImaging). Images were recorded with a Z-optical spacing of 2 µm and analyzed using the Image J software.

Progeny Assay

Sixteen L4-staged worms were individually placed on a 5cm NGM plate with op50. Every 24 hours, the worm was moved to a fresh plate for 10 consecutive days. 48 hours after

the original worm was removed from the plate, the number of living progeny was counted.

Cell Culture

MCF10A cells lines expressed a vector conferring puromycin/ blastocydin antibiotic resistance that was empty (control) or that drove the overexpression of Aurora B Kinase (AuBK OE). MCF10A cells were maintained in Dulbecco's modified Eagle's medium/F-12, phenol red free medium supplemented with 5% heat inactivated horse serum, 20 ng/ml recombinant EGF (Invitrogen), 0.5 µg/ml hydrocortisone (Sigma), 100 ng/ml cholera toxin (Sigma), and 10 µg/ml insulin (Sigma). U20S cells were maintained using Dulbecco's modified Eagle's medium with phenol red supplemented with 10% FBS.

siRNA knockdown

We used the following Thermo Scientific siRNAs: siGENOME Non-Targeting siRNA Pool#2 (D-001206-14-20), siGENOME Human NRDE2 (55051) siRNA- SMARTpool (M-013794-00-0005). siRNAs were added to the cell culture at a final concentration of 5nM in OPTIMEM Reduced Serum Media with Lipofectamine 2000 Reagent (1ug/ml final concentration) (Invitrogen) for 24 hours. Cells were then washed 1x with PBS and fresh MCF10A media was added. 48 hours after changing media, the cells were harvested for analysis.

Western Blot

Cultured cells were homogenized in Laemmli Buffer (60 mM Tris–HCl pH 7.6, 2% SDS, 1mM DTT) containing COMPLETE protease inhibitor cocktail (Roche #118361700001) and phosphatase inhibitors (Santa Cruz Biotechnology)). Protein concentrations were determined by performing DC Protein Assay (Bio-Rad) using BSA as standard. Protein extracts were resolved using Bolt 4%-12% Bis-Tris PAGE gels (Invitrogen) with 1x MES SDS Running Buffer (Life Technologies). Transfer to nitrocellulose membranes (Life Technologies) was performed on an iBlot apparatus (Invitrogen). Membranes were probed with primary antibodies overnight on a 4°C shaker and then incubated with horseradish peroxidase (HRP)-conjugated secondary antibodies, and signals were visualized with ECL (Bio-Rad) or Visualizer Western Blot Detection Kit, rabbit (Millipore). The following primary antibodies were used: GFP (Rockland, 600-101-215), phospho-Histone H3 (Ser10) (Cell Signaling Technologies, #9701), phospho-Histone H2A.X (Ser 139) (Cell Signaling Technologies, #9718), HA-tag (Cell Signaling Technologies #2367), PARP (Cell Signaling Technologies, #9542), β-actin HRP (Santa Cruz Biotechnology, sc-47778)

Cell Immunofluorescence

Cells were grown on a sterilized glass coverslip (Fisherbrand). After siRNA treatment, the cells were fixed with ice cold 100% methanol for 3 minutes at -20°C and rehydrated with TBST (1xTBS, 0.1% Tween 20). Antibodies were made up in blocking solution (2gBSA powder, 0.1g NaN3, 100mL TBST). The following primary antibodies were used: human anti-centromere (CREST, 1:50, Antibodies Incorporated 15-234) mouse anti-a-tubulin

(DM1a, 1:1000, Sigma T6199), rabbit anti-g-tubulin (1:1000, Sigma T3559). Cells were mounted with Vectashield Mounting Medium with DAPI (Vector Laboratories H-1200).

Time lapse Imaging

MCF10A cells expressing H2B::mCherry were imaged at 37°C with a 100x NA 1.49 objective lens (CFI APO TIRF; Nikon) on an inverted microscope system (TE2000 Perfect Focus System; Nikon) equipped with a Borealis modified spinning disk confocal unit (CSU10; Yokogawa) with 200-mW, 405 nm, 488 nm, 561 nm and 643 nm solid-state lasers (LMM5; Spectral Applied Research), electronic shutters, a Clara cooled scientific-grade interline CCD camera (Andor), and controlled by NIS-Elements software (Nikon).

Co-Immunoprecipitation

Cells were collected and lysed in cold lysis buffer (150mM NaCl/ 1.0% IGEPAL/ 50mM Tris-Cl (pH 7.4)) containing Complete protease inhibitor cocktail (Roche, 118361700001) by nutating at 4°C for 30 minutes. The lysate was spun at 14K G, and supernatant was transferred to a new tube, and cleared using 50ul of Dynabeads Protein A (Invitrogen, 10001D). Pre-cleared lysate was removed from the beads using magnetic separation (input sample was collected at this stage), added to 5 ul of anti-GFP antibody (Rockland, 600-101-215), and nutated at 4°C for 2 hours. Antibody-protein complexes were isolated by the addition of Dynabeads Protein A (Invitrogen, 10001D), overnight nutation and magnetic separation. The beads were washed with the lysis buffer

414 containing protease inhibitors five times. IP western blot bands were normalized to 5%
415 sample input.
416
417 **Acknowledgements**
418 Thanks to Dr. Scott Kennedy for providing the nrde-2 (gg91) strain and to Dr. Needhi
419 Bhalla (UC Santa Cruz) for providing the CED-1::GFP strain. We would like to thank Dr.
420 Gina Caldas (Dernburg lab at UC Berkeley) for reagents and advice about *C. elegans*
421 gonad immunofluorescence staining. We extend a special thanks to Christina Hueschen
422 (Dumont lab at UCSF) for creating a nuclear GFP quantification MatLab script. We would
423 also like to thank Dr. Sophie Dumont and Dr. Torsten Wittmann (UCSF) for use of their
424 microscopes and advice regarding imaging and the cell cycle.
425
426 **Funding**
427 Noelle L'Etoile and Andrei Goga are supported in part through funds from the National
428 Institutes of Health Research Program—Cooperative Agreements (U19CA179512-05S2).
429 Dr. Andrei Goga and Aarati Asundi is also receive funding support from the CDMRP BCRP
430 (W81XWH-12-1-0272) and NIH (U19CA179512). Dr. Stephen N. Floor and Dr. Srivats
431 Venkataramanan are supported by funds from the California Tobacco-Related Disease
432 Research Grants Program Office of the University of California, 27KT-0003 and the
433 Program for Breakthrough Biomedical Research, which is partially funded by the Sandler
434 Foundation. Dr. Gina Caldas Cuellar is supported by the PEW Latin American
435 Fellow program and the Damon Runyon Fellowship.

436

437 **References**

438 [1] Buckley BA, Burkhart KB, Gu SG, Spracklin G, Kershner A, Fritz H, Kimble J, Fire A,

439 Kennedy S. A nuclear Argonaute promotes multigenerational epigenetic inheritance and

440 germline immortality. Nature. 2012 Sep 20;489(7416):447-51. doi:

441 10.1038/nature11352.

442

443 [2] Burton NO, Burkhart KB, Kennedy S. Nuclear RNAi maintains heritable gene silencing

444 in *Caenorhabditis elegans*. Proc Natl Acad Sci U S A. 2011 Dec 6;108(49):19683-8. doi:

445 10.1073/pnas.1113310108.

446

447 [3] Zhou Z, Hartwieg E, Horvitz HR. CED-1 is a transmembrane receptor that mediates

448 cell corpse engulfment in *C. elegans*. Cell. 2001 Jan 12;104(1):43-56.

449

450 [4] Soule HD, Maloney TM, Wolman SR, Peterson WD Jr, Brenz R, McGrath CM, Russo J,

451 Pauley RJ, Jones RF, Brooks SC. Isolation and characterization of a spontaneously

452 immortalized human breast epithelial cell line, MCF-10. Cancer Res. 1990 Sep

453 15;50(18):6075-86.

454

455 [5] Goto H, Yasui Y, Nigg EA, Inagaki M. Aurora-B phosphorylates Histone H3 at serine28

456 with regard to the mitotic chromosome condensation. Genes Cells. 2002 Jan;7(1):11-7.

457

458 [6] Lampson MA, Grishchuk EL. Mechanisms to Avoid and Correct Erroneous
459 Kinetochore-Microtubule Attachments. Biology (Basel). 2017 Jan 5;6(1). pii: E1. doi:
460 10.3390/biology6010001.
461
462 [7] Welburn JP, Vleugel M, Liu D, Yates JR 3rd, Lampson MA, Fukagawa T, Cheeseman
463 IM. Aurora B phosphorylates spatially distinct targets to differentially regulate the
464 kinetochore-microtubule interface. Mol Cell. 2010 May 14;38(3):383-92. doi:
465 10.1016/j.molcel.2010.02.034.
466
467 [8] Steigemann P, Wurzenberger C, Schmitz MH, Held M, Guizetti J, Maar S, Gerlich DW.
468 Aurora B-mediated abscission checkpoint protects against tetraploidization. Cell. 2009
469 Feb 6;136(3):473-84. doi: 10.1016/j.cell.2008.12.020.
470
471 [9] Fell VL, Walden EA, Hoffer SM, Rogers SR, Aitken AS, Salemi LM, Schild-Poulter C.
472 Ku70 Serine 155 mediates Aurora B inhibition and activation of the DNA damage
473 response. Sci Rep. 2016 Nov 16;6:37194. doi: 10.1038/srep37194.
474
475 [10] Monaco L, Kolthur-Seetharam U, Loury R, Murcia JM, de Murcia G, Sassone-Corsi P.
476 Inhibition of Aurora-B kinase activity by poly(ADP-ribosyl)ation in response to DNA
477 damage. Proc Natl Acad Sci U S A. 2005 Oct 4;102(40):14244-8.
478

[11] Guang S, Bochner AF, Burkhart KB, Burton N, Pavelec DM, Kennedy S. Small regulatory RNAs inhibit RNA polymerase II during the elongation phase of transcription. Nature. 2010 Jun 24;465(7301):1097-101. doi: 10.1038/nature09095.

[12] Chieffi P. Aurora B: A new promising therapeutic target in cancer. Intractable Rare Dis Res. 2018 May;7(2):141-144. doi: 10.5582/irdr.2018.01018.

[13] Tang A, Gao K, Chu L, Zhang R, Yang J, Zheng J. Aurora kinases: novel therapy targets in cancers. Oncotarget. 2017 Apr 4;8(14):23937-23954. doi: 10.18632/oncotarget.14893.

[14] Zuazua-Villar P, Rodriguez R, Gagou ME, Eyers PA, Meuth M. DNA replication stress in CHK1-depleted tumour cells triggers premature (S-phase) mitosis through inappropriate activation of Aurora kinase B. Cell Death Dis. 2014 May 22;5:e1253. doi: 10.1038/cddis.2014.231.

[15] Kabeche L, Nguyen HD, Buisson R, Zou L. A mitosis-specific and R loop-driven ATR pathway promotes faithful chromosome segregation. Science. 2018 Jan 5;359(6371):108-114. doi: 10.1126/science.aan6490.

[16] Sakaguchi A, Sarkies P, Simon M, Doebley AL, Goldstein LD, Hedges A, Ikegami K, Alvares SM, Yang L, LaRocque JR, Hall J, Miska EA, Ahmed S. *Caenorhabditis elegans*

RSD-2 and RSD-6 promote germ cell immortality by maintaining small interfering RNA populations. Proc Natl Acad Sci U S A. 2014 Oct 14;111(41):E4323-31. doi: 10.1073/pnas.1406131111.

[17] Aronica L, Kasparek T, Ruchman D, Marquez Y, Cipak L, Cipakova I, Anrather D, Mikolaskova B, Radtke M, Sarkar S, Pai CC, Blaikley E, Walker C, Shen KF, Schroeder R, Barta A, Forsburg SL, Humphrey TC. The spliceosome-associated protein Nrl1 suppresses homologous recombination-dependent R-loop formation in fission yeast. Nucleic Acids Res. 2016 Feb 29;44(4):1703-17. doi: 10.1093/nar/gkv1473.

[18] Conine CC, Moresco JJ, Gu W, Shirayama M, Conte D Jr, Yates JR 3rd, Mello CC. Argonautes promote male fertility and provide a paternal memory of germline gene expression in *C. elegans*. Cell. 2013 Dec 19;155(7):1532-44. doi: 10.1016/j.cell.2013.11.032.

[19] van Wolfswinkel JC, Claycomb JM, Batista PJ, Mello CC, Berezikov E, Ketting RF. CDE-1 affects chromosome segregation through uridylation of CSR-1-bound siRNAs. Cell. 2009 Oct 2;139(1):135-48. doi: 10.1016/j.cell.2009.09.012.

[20] Mao H, Zhu C, Zong D, Weng C, Yang X, Huang H, Liu D, Feng X, Guang S. The Nrde Pathway Mediates Small-RNA-Directed Histone H3 Lysine 27 Trimethylation in

522 *Caenorhabditis elegans*. Curr Biol. 2015 Sep 21;25(18):2398-403. doi:
523 10.1016/j.cub.2015.07.051.
524
525 [21] Burkhart KB, Guang S, Buckley BA, Wong L, Bochner AF, Kennedy S. A pre-mRNA-
526 associating factor links endogenous siRNAs to chromatin regulation. PLoS Genet. 2011
527 Aug;7(8):e1002249. doi: 10.1371/journal.pgen.1002249.
528
529 [22] Richard P, Ogami K, Chen Y, Feng S, Moresco JJ, Yates JR 3rd, Manley JL. NRDE-2,
530 the human homolog of fission yeast Nrl1, prevents DNA damage accumulation in human
531 cells. RNA Biol. 2018 Aug 2:1-9. doi: 10.1080/15476286.2018.1467180.
532
533 [23] Lin YC, Boone M, Meuris L, Lemmens I, Van Roy N, Soete A, Reumers J, Moisse M,
534 Plaisance S, Drmanac R, Chen J, Speleman F, Lambrechts D, Van de Peer Y, Tavernier J,
535 Callewaert N. Genome dynamics of the human embryonic kidney 293 lineage in
536 response to cell biology manipulations. Nat Commun. 2014 Sep 3;5:4767. doi:
537 10.1038/ncomms5767.
538
539 [24] Bylund L, Kytölä S, Lui WO, Larsson C, Weber G. Analysis of the cytogenetic stability
540 of the human embryonal kidney cell line 293 by cytogenetic and STR profiling
541 approaches. Cytogenet Genome Res. 2004;106(1):28-32.
542

543 [25] Belin BJ, Lee T, Mullins RD. DNA damage induces nuclear actin filament assembly by
544 Formin -2 and Spire-½ that promotes efficient DNA repair. [corrected]. Elife. 2015 Aug
545 19;4:e07735. doi: 10.7554/eLife.07735. Erratum in: Elife. 2015;4. doi:
546 10.7554/eLife.11935.
547
548 [26] Caridi CP, D'Agostino C, Ryu T, Zapotoczny G, Delabaere L, Li X, Khodaverdian VY,
549 Amaral N, Lin E, Rau AR, Chiolo I. Nuclear F-actin and myosins drive relocalization of
550 heterochromatic breaks. Nature. 2018 Jul;559(7712):54-60. doi: 10.1038/s41586-018-
551 0242-8.
552
553 [27] Kim asutis KM, Kozminski KG. Cell cycle checkpoint regulators reach a zillion. Cell
554 Cycle. 2013 May 15;12(10):1501-9. doi: 10.4161/cc.24637.
555
556 [28] Hamperl S, Cimprich KA. Conflict Resolution in the Genome: How Transcription and
557 Replication Make It Work. Cell. 2016 Dec 1;167(6):1455-1467. doi:
558 10.1016/j.cell.2016.09.053.
559
560 [29] Segil N, Guermah M, Hoffmann A, Roeder RG, Heintz N. Mitotic regulation of TFIID:
561 inhibition of activator-dependent transcription and changes in subcellular localization.
562 Genes Dev. 1996 Oct 1;10(19):2389-400.
563

564 [30] Taylor WR, Stark GR. Regulation of the G2/M transition by p53. Oncogene. 2001
565 Apr 5;20(15):1803-15.
566
567 [31] Kimble J, Simpson P. The LIN-12/Notch signaling pathway and its regulation. Annu
568 Rev Cell Dev Biol. 1997;13:333-61.
569
570 [32] Fox PM, Schedl T. Analysis of Germline Stem Cell Differentiation Following Loss of
571 GLP-1 Notch Activity in *Caenorhabditis elegans*. Genetics. 2015 Sep;201(1):167-84. doi:
572 10.1534/genetics.115.178061.
573
574 [33] Dalfó D, Michaelson D, Hubbard EJ. Sensory regulation of the *C. elegans* germline
575 through TGF-β-dependent signaling in the niche. Curr Biol. 2012 Apr 24;22(8):712-9. doi:
576 10.1016/j.cub.2012.02.064.
577
578 [34] Michaelson D, Korta DZ, Capua Y, Hubbard EJ. Insulin signaling promotes germline
579 proliferation in *C. elegans*. Development. 2010 Feb;137(4):671-80. doi:
580 10.1242/dev.042523. Erratum in: Development. 2014 Jan;141(1):237.
581
582 [35] Begasse ML, Leaver M, Vazquez F, Grill SW, Hyman AA. Temperature Dependence
583 of Cell Division Timing Accounts for a Shift in the Thermal Limits of *C. elegans* and
584 *C. briggsae*. Cell Rep. 2015 Feb 4. pii: S2211-1247(15)00007-8. doi:
585 10.1016/j.celrep.2015.01.006.

[36] Claycomb JM, Batista PJ, Pang KM, Gu W, Vasale JJ, van Wolfswinkel JC, Chaves DA, Shirayama M, Mitani S, Ketting RF, Conte D Jr, Mello CC. The Argonaute CSR-1 and its 22G-RNA cofactors are required for holocentric chromosome segregation. Cell. 2009 Oct 2;139(1):123-34. doi: 10.1016/j.cell.2009.09.014.

[37] Vought VE, Ohmachi M, Lee MH, Maine EM. EGO-1, a putative RNA-directed RNA polymerase, promotes germ line proliferation in parallel with GLP-1/notch signaling and regulates the spatial organization of nuclear pore complexes and germ line P granules in *Caenorhabditis elegans*. Genetics. 2005 Jul;170(3):1121-32.

[38] Maine EM, Hauth J, Ratliff T, Vought VE, She X, Kelly WG. EGO-1, a putative RNA-dependent RNA polymerase, is required for heterochromatin assembly on unpaired dna during *C. elegans* meiosis. Curr Biol. 2005 Nov 8;15(21):1972-8.

[39] Duchaine TF, Wohlschlegel JA, Kennedy S, Bei Y, Conte D Jr, Pang K, Brownell DR, Harding S, Mitani S, Ruvkun G, Yates JR 3rd, Mello CC. Functional proteomics reveals the biochemical niche of *C. elegans* DCR-1 in multiple small-RNA-mediated pathways. Cell. 2006 Jan 27;124(2):343-54.

606 [40] Sy Bukhari SI, Vasquez-Rifo A, Gagné D, Paquet ER, Zetka M, Robert C, Masson JY,
607 Simard MJ. The microRNA pathway controls germ cell proliferation and differentiation in
608 *C. elegans*. Cell Res. 2012 Jun;22(6):1034-45. doi: 10.1038/cr.2012.31.
609
610 [41] Rocheleau CE, Cullison K, Huang K, Bernstein Y, Spilker AC, Sundaram MV. The
611 *Caenorhabditis elegans* ekl (enhancer of ksr-1 lethality) genes include putative
612 components of a germline small RNA pathway. Genetics. 2008 Mar;178(3):1431-43. doi:
613 10.1534/genetics.107.084608.
614
615 [42] Menck CF, Munford V. DNA repair diseases: What do they tell us about cancer and
616 aging? Genet Mol Biol. 2014 Mar;37(1 Suppl):220-33.
617
618 [43] Lubas M, Christensen MS, Kristiansen MS, Domanski M, Falkenby LG, Lykke-
619 Andersen S, Andersen JS, Dziembowski A, Jensen TH. Interaction profiling identifies the
620 human nuclear exosome targeting complex. Mol Cell. 2011 Aug 19;43(4):624-37. doi:
621 10.1016/j.molcel.2011.06.028.
622
623 [44] Ogami K, Richard P, Chen Y, Hoque M, Li W, Moresco JJ, Yates JR 3rd, Tian B,
624 Manley JL. An Mtr4/ZFC3H1 complex facilitates turnover of unstable nuclear RNAs to
625 prevent their cytoplasmic transport and global translational repression. Genes Dev.
626 2017 Jun 15;31(12):1257-1271. doi: 10.1101/gad.302604.117.
627

628 [45] Virtanen JA, Vartiainen MK. Diverse functions for different forms of nuclear actin.
629 Curr Opin Cell Biol. 2017 Jun;46:33-38. doi: 10.1016/j.ceb.2016.12.004.
630
631 [46] Barnum KJ, O'Connell MJ. Cell cycle regulation by checkpoints. Methods Mol Biol.
632 2014;1170:29-40. doi: 10.1007/978-1-4939-0888-2_2.
633
634 [47] McMurchy AN, Stempor P, Gaarenstroom T, et al. A team of heterochromatin
635 factors collaborates with small RNA pathways to combat repetitive elements and
636 germline stress. Heard E, ed. eLife. 2017;6:e21666. doi:10.7554/eLife.21666.
637
638 [48] Hamperl S, Cimprich KA. Conflict Resolution in the Genome: How Transcription and
639 Replication Make It Work. Cell. 2016 Dec 1;167(6):1455-1467. doi:
640 10.1016/j.cell.2016.09.053.
641
642 [49] Larson AG, Elnatan D, Keenen MM, Trnka MJ, Johnston JB, Burlingame AL, Agard
643 DA, Redding S, Narlikar GJ. Liquid droplet formation by HP1α suggests a role for phase
644 separation in heterochromatin. Nature. 2017 Jul 13;547(7662):236-240. doi:
645 10.1038/nature22822.

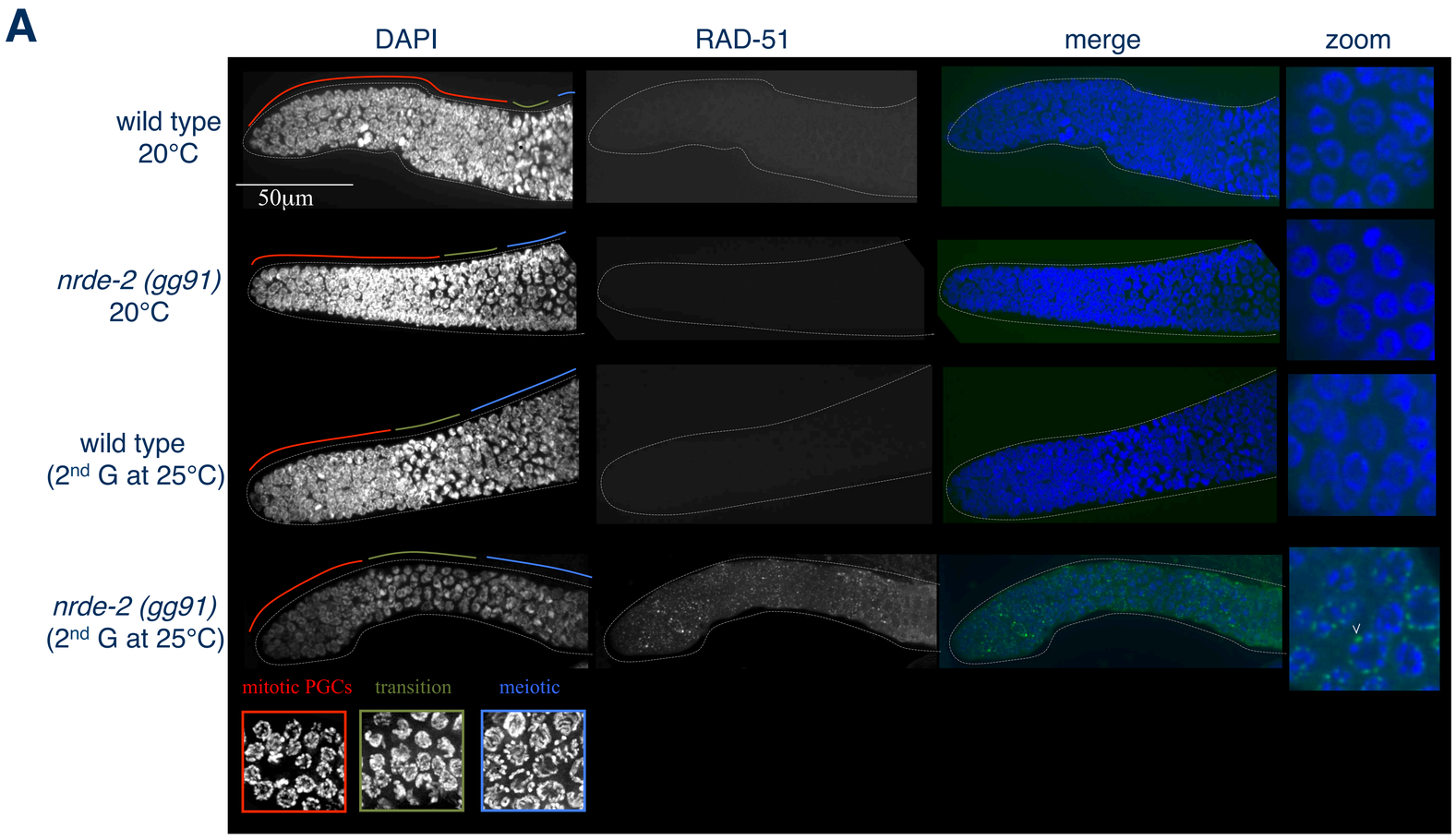

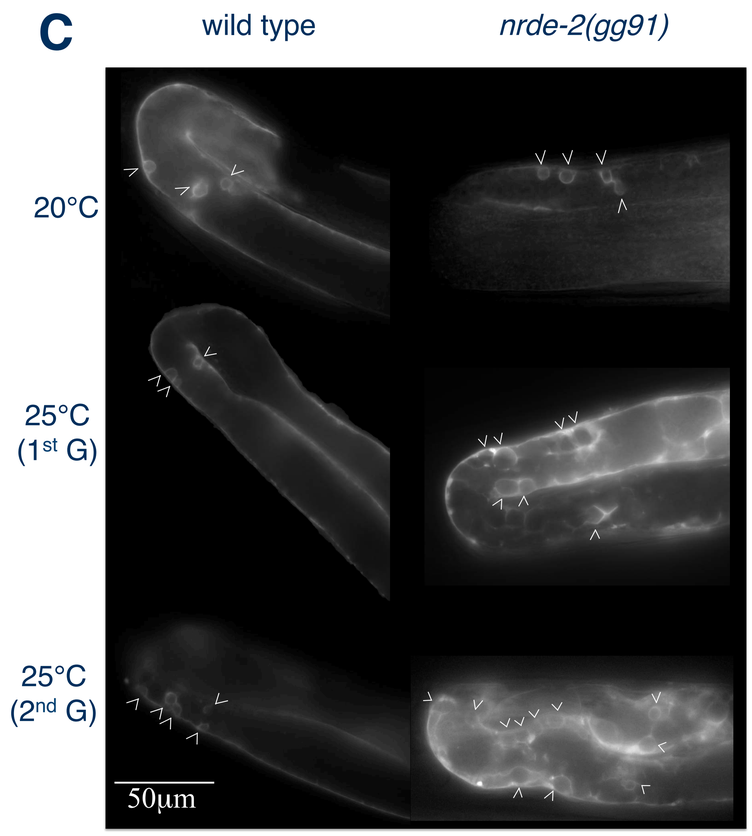

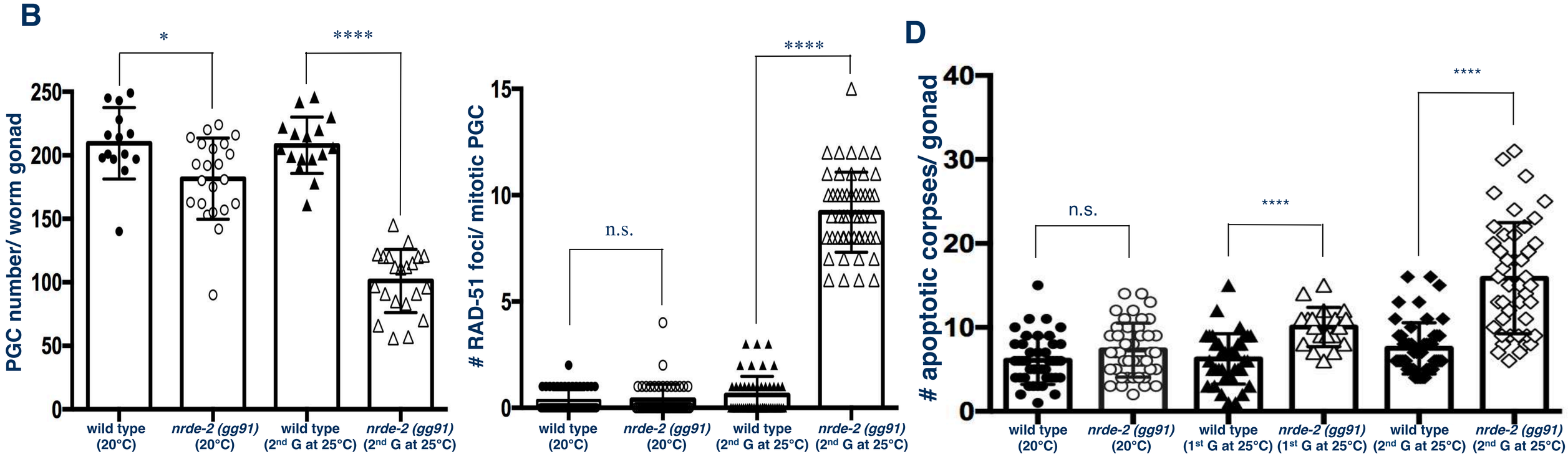

Figure 1A: Loss of NRDE-2 significantly decreases the number of mitotic germ cells and increases the accumulation of RAD-51 foci in these cells in worms grown for two generations at 25°C. Maximum intensity projections of DAPI stained gonads with RAD-51 foci visualized in the green channel using an antibody against RAD-51. (Left panels) The red line indicates mitotic proliferating germ cell zone, the green line indicates transition zone where DAPI labeled chromosomes exhibit a "crescent-like" morphology, and the blue line indicates meiotic zone. (Right panels) Zoomed in image of one focal plane of mitotic PGCs. The white arrow indicates a single RAD-51puncta. **Figure 1B: (Left Panel) Loss of NRDE-2 at 20°C decreases the number of PGCs and this is exacerbated when the worms are grown for two generations at 25°C.** Mean number ± SEM of PCGs in gonads of wild type propagated at 20°C (209.6 ± 7.518, n=14) and *nrde-2(gg91)* mutants propagated at 20°C (181.6 ± 6.830, n=22) are different (*p=0.0115). PGCs of G2 wild type worms propagated at 25°C (207.9 ± 5.542, n=16) and G2 *nrde-2(gg91)* mutants propagated at 25°C (101.0 ± 5.418, n=21) is different (****p<0.0001). **(Right panel) Loss of NRDE2 at 25°C increases the number of RAD-51 foci per PGC nucleus.** The focal plane with the greatest number of RAD-51 foci was chosen for each germ cell nucleus. The number of RAD-51 foci per nuclear focal plane cell were averaged across 50 mitotic PGCs (10 PGCs closest to the distal tip cell in 5 gonads per condition). Mean number ± SEM of RAD-51 foci in gonads of wild type propagated at 20°C (0.3400 ± 0.07346, n=50) and *nrde-2(gg91)* mutants propagated at 20°C (0.3800 ± 0.1026, n=50) are not different. RAD-51 foci of G2 wild type worms propagated at 25°C (0.6000 ± 0.1245, n=50) have more RAD-51 foci than G2 *nrde-2(gg91)* mutants propagated at 25°C (9.200 ± 0.2665, n=50, ****p<0.0001). All data represents 3 experimental days and the p-values were determined using unpaired Student's t test. **Figure 1C: Loss of NRDE-2 increases the number of CED-1::GFP-labeled cell corpses in worms grown for 1 or 2 generations at 25°C.** CED-1::GFP expressed in *nrde-2(gg91)* and wild type *C. elegans* gonads (white arrows indicate apoptotic cell corpses). **Figure 1D: Loss of NRDE-2 increases the number of apoptotic corpses in the gonads of worms grown for 1 or 2 generations at 25°C.** Quantification of CED-1::GFP labeled germ cells. Wild type worms propagated at 20°C (6.071 ± 0.4409, n=42) have the same number of corpses as *nrde-2(gg91) mutants propogated* at 20°C (7.302 ± 0.4897, n=43). Wild type worms (6.263 ± 0.4869, n=38) have fewer cell corpses than *nrde-2(gg91)* mutants when grown for 1 generation at 25°C (10.05 ± 0.5379, n=19, ****p<0.0001). Wild type worms (7.510 ± 0.4278, n=51) have fewer cell corpses than *nrde-2 (gg91*) mutants when grown for 2 generations at 25°C (15.86 ± 0.9987, n=44, ****p<0.0001). Cell corpses identified as described in Figure 1D. Data represents 3 experimental days and the p-values were determined using unpaired Student's t test.

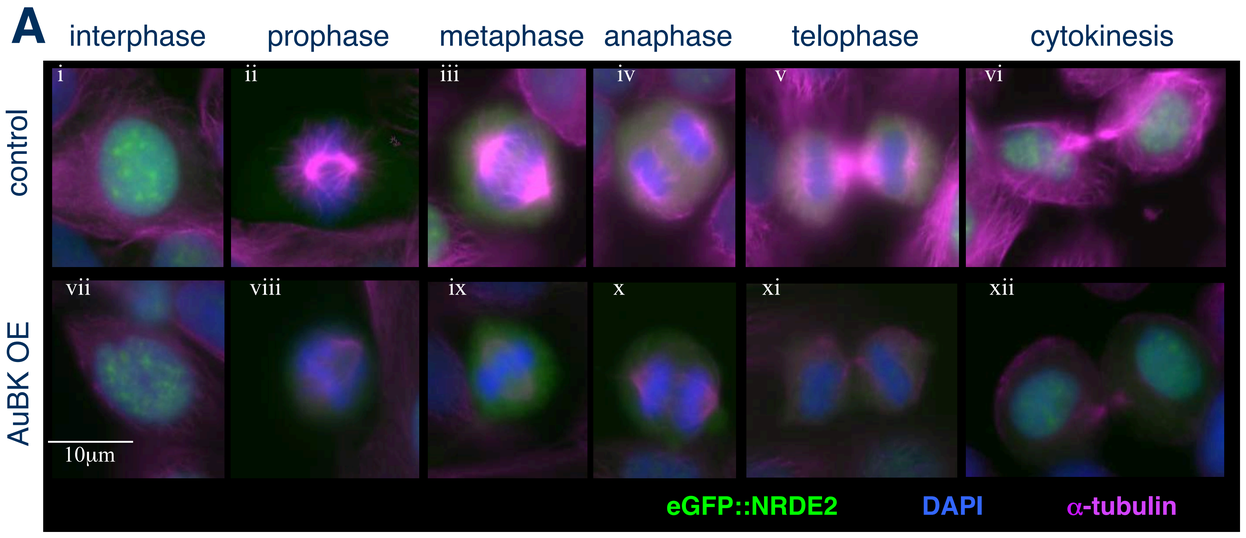

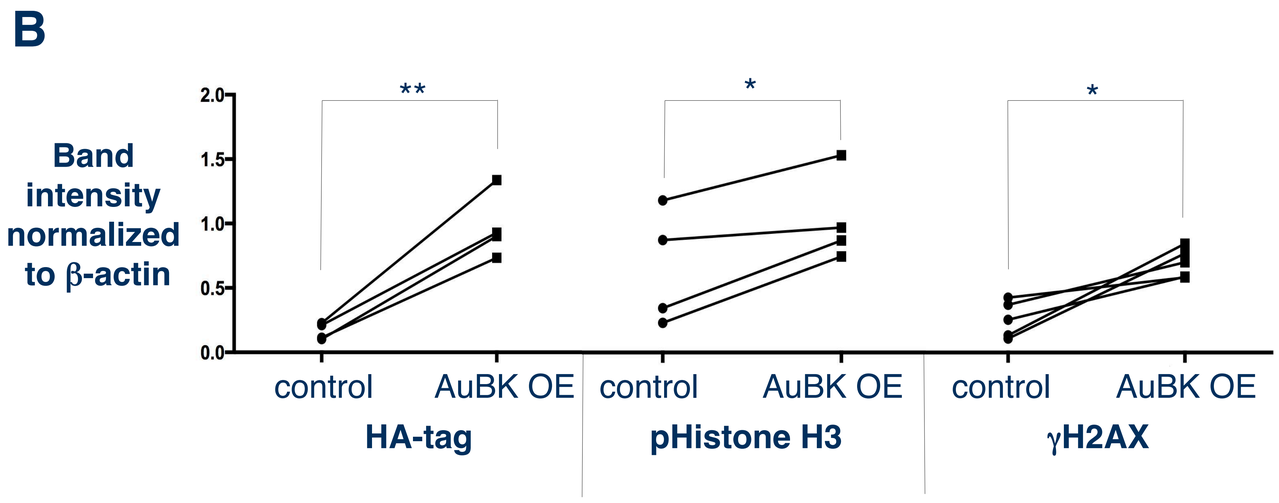

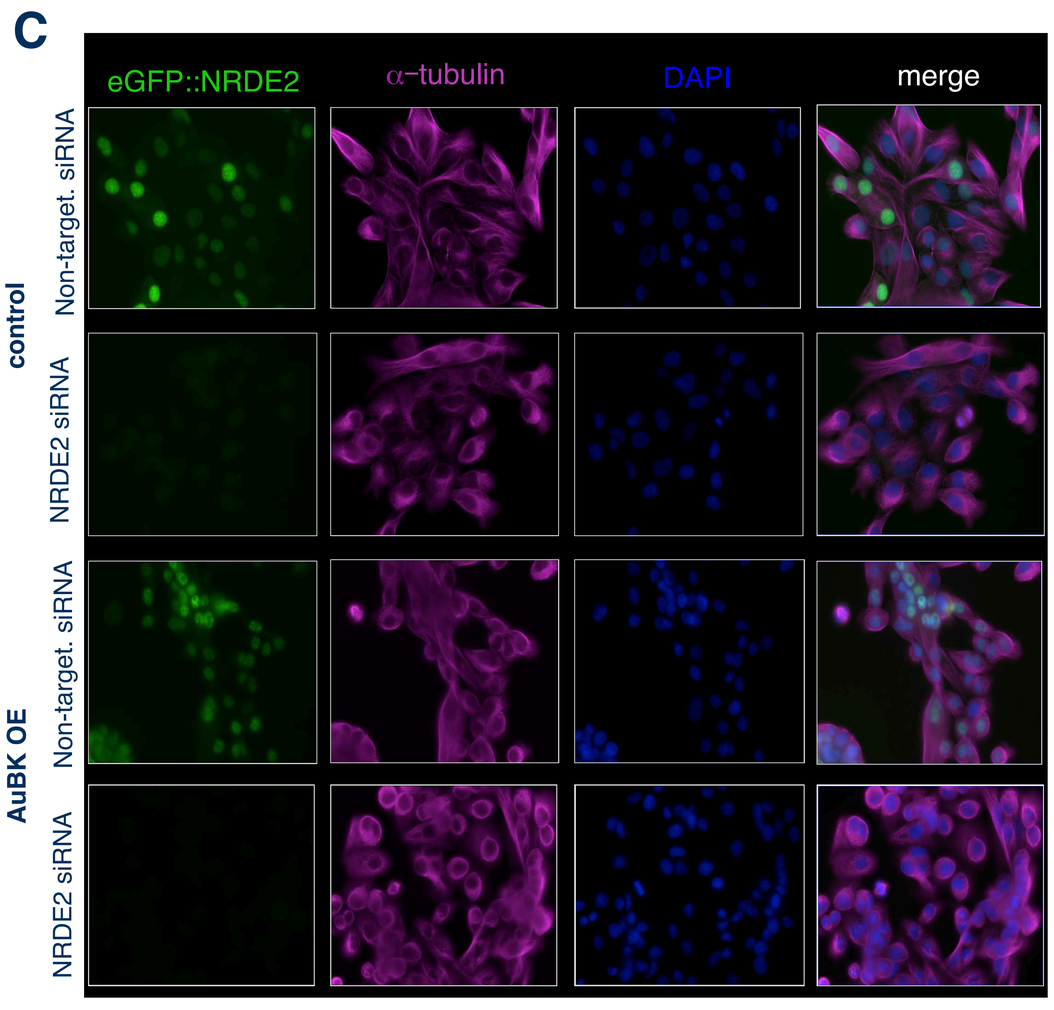

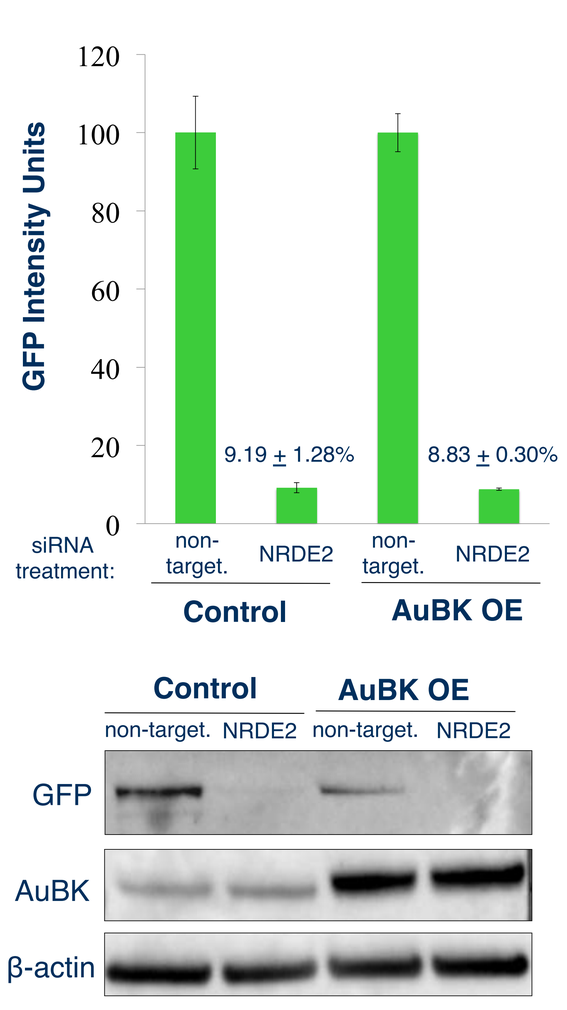

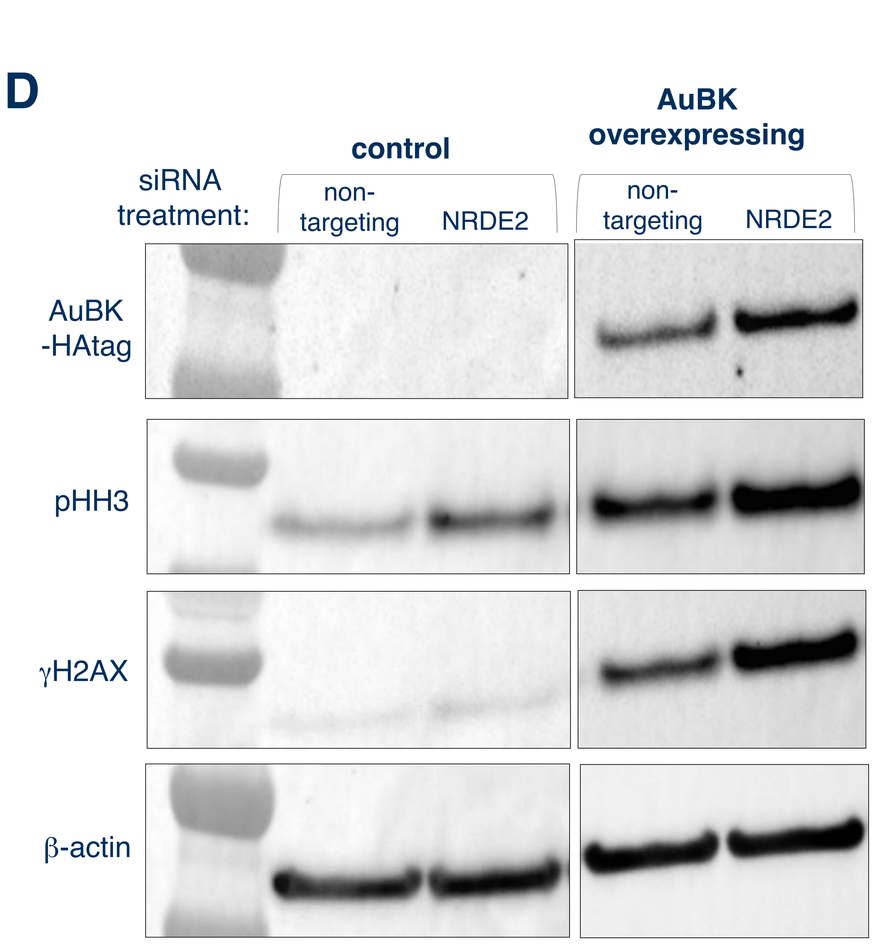

Figure 2A: In MCF10A human breast cells with endogenous or overexpressed AuBK levels, eGFP-NRDE2 localizes to puncta within the nucleus when chromatin is de-condensed during interphase and cytokinesis. In each circumstance, eGFP-NRDE2 is diffuse throughout all other stages of mitosis. Epifluorescent images of cells expressing eGFP-tagged NRDE2 as visualized in the green channel, chromatin as visualized by DAPI staining in the blue and the cytoskeleton as visualized by an antibody against α-tubulin in the Cy5 (far red) channel. (Top row) MCF10A cells expressing control vector. (Bottom row) MCF10A cells over-expressing AuBK. **Figure 2B: AuBK overexpression in MCF10A cells as a means to stress cells by increasing basal levels of DNA damage.** Western blot band intensities (see figure 2D for representative blot) were measured and normalized to β-actin band intensity. HA-tag band intensity in HA-tagged AUBK overexpressing cells is higher than in control cells (n=4; p=0.0046). Phosphorylated Histone H3 band intensity in AUBK overexpressing cells is higher than in control cells (n=4; p=0.0337). Phosphorylated H2AX band intensity in AUBK overexpressing cells is higher than in control cells (n=5; p=0.0146). All p-values determined by paired Student's t test. **Figure 2C: Average GFP intensity in MCF10A cells expressing eGFP-tagged NRDE2 decreases specifically in cells treated with NRDE2 targeted siRNA.** (Left) Epifluorescent images of MCF10A cells expressing eGFP-tagged NRDE2 as visualized in the green channel, the cytoskeleton as visualized by an antibody against α-tubulin in the far red channel and DNA as visualized by DAPI staining in the blue channel. Control or AuBK overexpressing MCF10A cells were treated with non-targeting siRNA or NRDE2 siRNA. (Top right) Quantification of epifluorescent GFP intensity of control and AuBK overexpressing cells treated with NRDE2 siRNA and normalized to the respective non-targeting siRNA treated cells. (Bottom right) Representative western blot using anti-GFP to detect eGFP-tagged NRDE2 inMCF10A cells treated with non-targeting or NRDE2 targeted siRNA. All cells treated with siRNA for 72 hours before imaging. Data represents 4 experimental days. **Figure 2D: MCF10A cells that overexpress HA-tagged AuBK show an increase in phosphorylated Histone H3 and an increase in the DNA damage marker γH2AX.** Representative blot: Anti-HA-tag used to detect AuBK in cells transformed with AuBK-HAtag in MCF10A cells. AuBK overexpressing cells have increased levels of phosphorylated Histone H3 and increased levels of γH2AX expression as compared to control cells. Western blot band intensities were measured and normalized to β-actin band intensity. See Fig S3 for quantification and statistics.

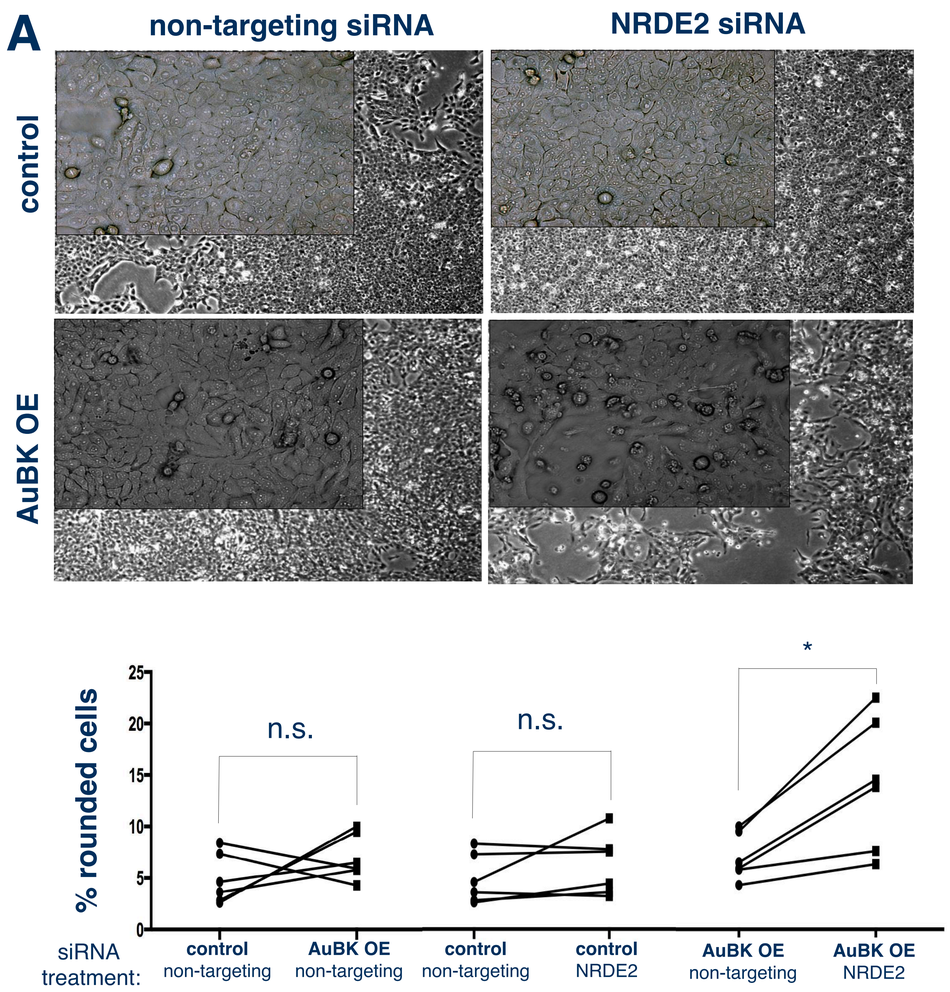

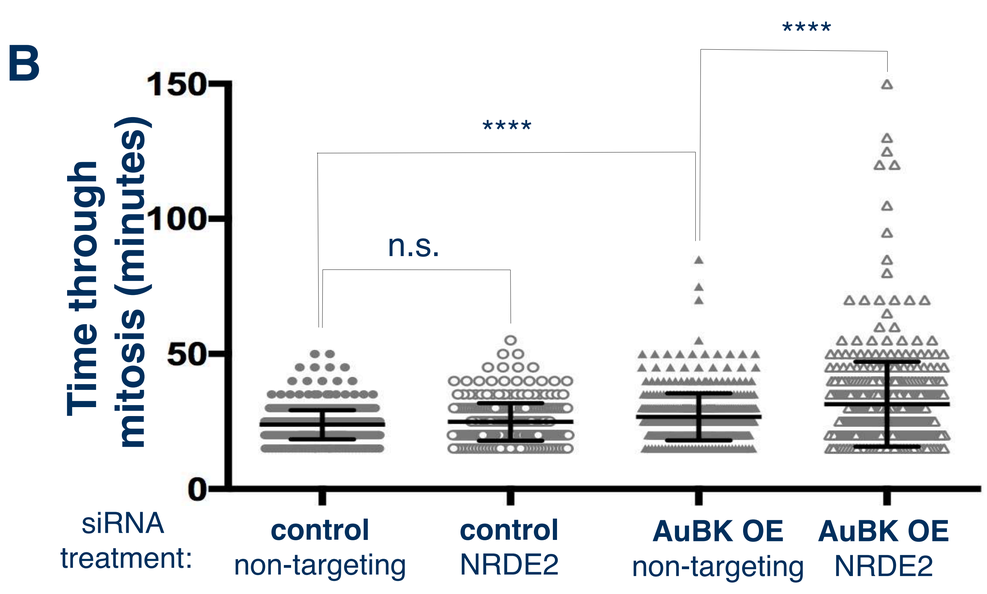

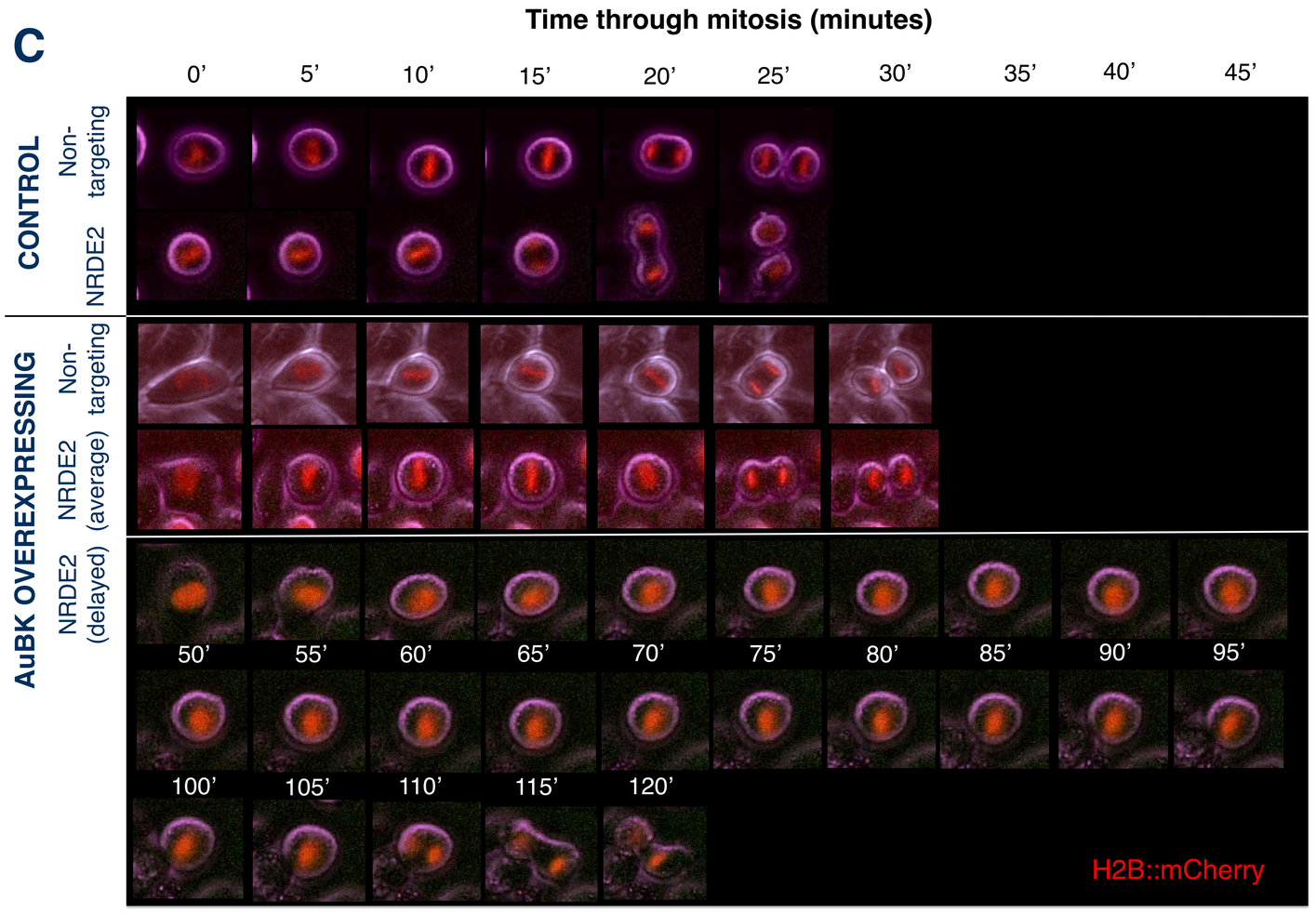

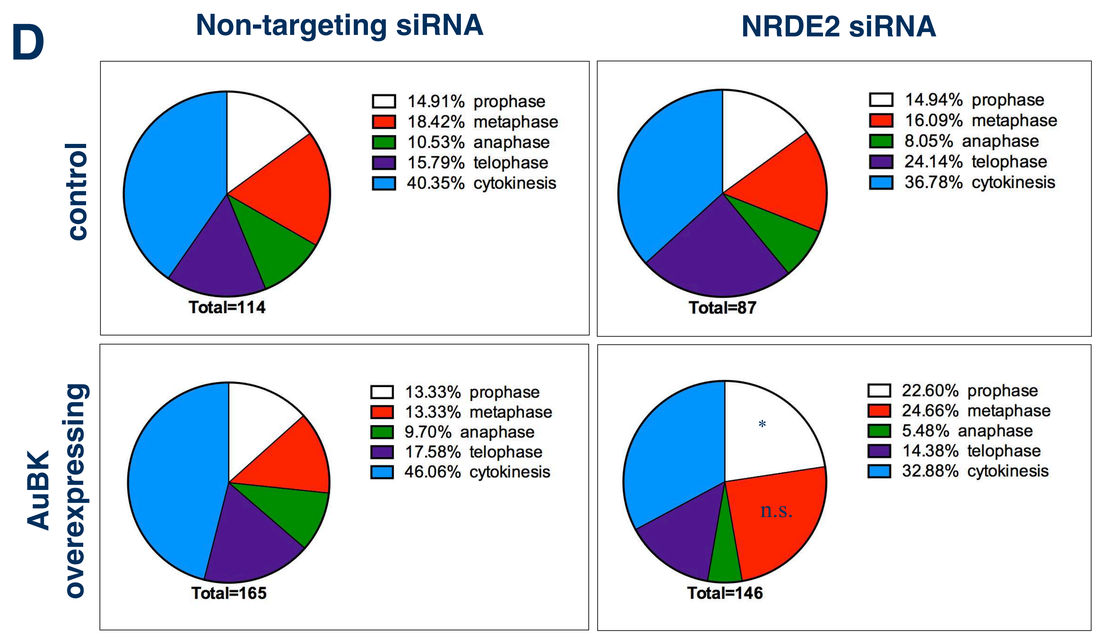

Figure 3A: Loss of NRDE2 in MCF10A cells overexpressing AuBK results in an increase in the percentage of cells with a rounded morphology. (Top) Brightfield images of cells 72 hours after siRNA treatment taken with 4x objective and 20x objective (inset). (Bottom) Quantitation of cell morphology. (Left paired points) Control or AuBK OE MCF10A cells show no difference in the percentage of round cells in cultures treated with non-targeting siRNA. (Middle paired points) MCF10A control cells show no difference in the percentage of round cells upon NRDE2 siRNA treatment as compared to non-targeting siRNA treatment. (Right paired points) MCF10A AuBK OE cells show a significant increase (*p=0.0110) in the percentage of round cells upon NRDE2 siRNA treatment as compared to non-targeting siRNA treatment. Data represents 6 experimental days. All p-values determined by paired Student's t test. **Figure 3B: Loss of NRDE2 in MCF10A cells overexpressing AuBK delays time through mitosis.** Time required for individual MCF10A cells to through mitosis. Control cells treated with NRDE2 siRNA (24.87 ± 0.3902, n=318) do not take significantly longer than control cells treated with non-targeting siRNA (23.79 ± 0.2442, n=492) to progrss through mitosis (p=not significant, Mann-Whitney test). AuBK over-expressing cells treated with NRDE2 siRNA (31.40 ± 0.7220, n=472) take significantly longer than cell trated with non-targeting siRNA (26.72 ± 0.4120, n=451) to progress through mitosis (****p<0.0001, Mann-Whitney test) **Figure 3C: Loss of NRDE delays time through mitosis in a subset of MCF10A cells overexpressing AuBK** of live MCF10A cells expressing H2B::mCherry visualized in the red channel to visualize chromatin compaction and chromosome separation. **Figure 3D: Loss of NRDE2 in AuBK overexpressing MCF10A cells significantly increases the proportion of cells in prophase.** Quantification of the percentage of cells in each phase of mitosis shows that AuBK overexpressing MCF10A cells have significantly more cells in prophase after treatment with NRDE2 siRNA as compared to treatment with non-targeting siRNA (p= 0.0258, determined by student's t test). Data represents 4 experimental days.

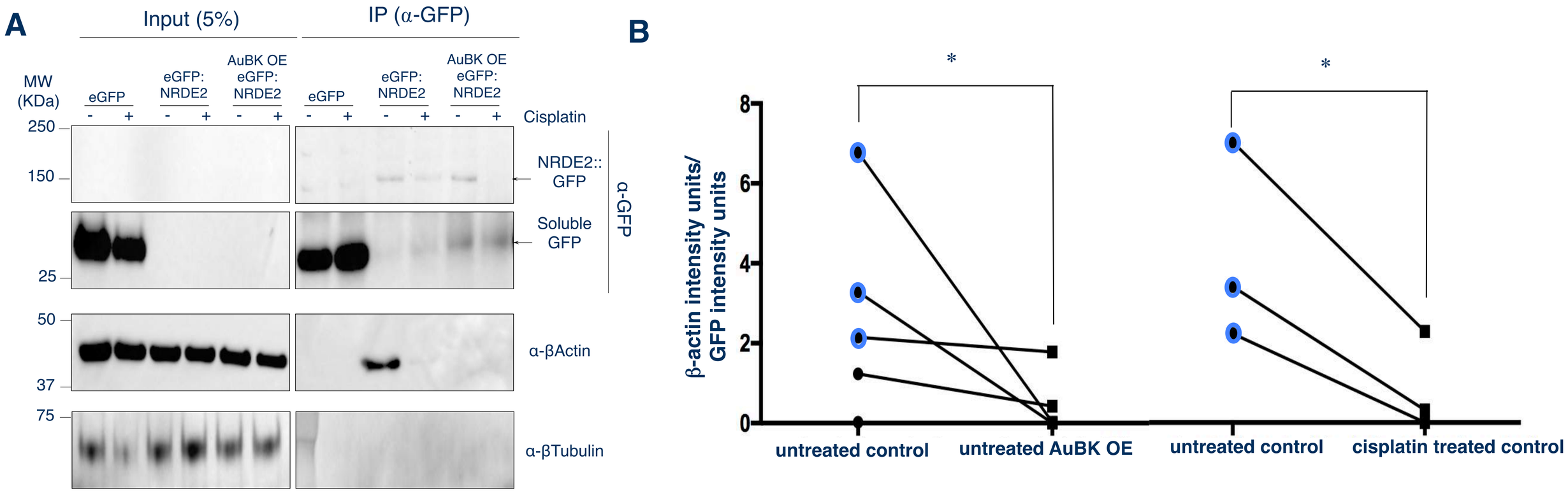

Figure 4A: eGFP::NRDE2 interacts with β-actin in control cells. This interaction is weakened in AuBK OE cells and when cells are treated with cisplatin. Representative western blots of MCF10A cell lysates. MCF10A cells were treated with 60uM cisplatin for 16 hours. Co-IP was performed using goat Anti-GFP antibody to pull down eGFP::NRDE2 from MCF10A cell lysates. Western blots were developed using rabbit anti-GFP polyclonal antibody to detect eGFP::NRDE2 and soluble GFP, anti-β-actin HRP antibody and mouse anti-β-tubulin antibody (negative control). **Figure 4B: The amount of β-actin per unit of IP'd GFP::NRDE2 decreases when DNA damage is induced in cells by AuBK OE or by cisplatin drug treatment.** (Left) The amount of β-actin per unit of co-IP'd eGFP::NRDE2 decreases when MCF10A cells overexpress AuBK as compared to MCF10A control cells (*Permutation test exact p-value =0.036). (Right) The amount of β-actin per unit of co-IP'd eGFP::NRDE2 decreases when MCF10A control cells are treated with 60uM cisplatin as compared to untreated control MCF10A cells. (*p-value =0.045 as assessed by paired student's t test). Note: Blue data points represent quantification of the same samples.

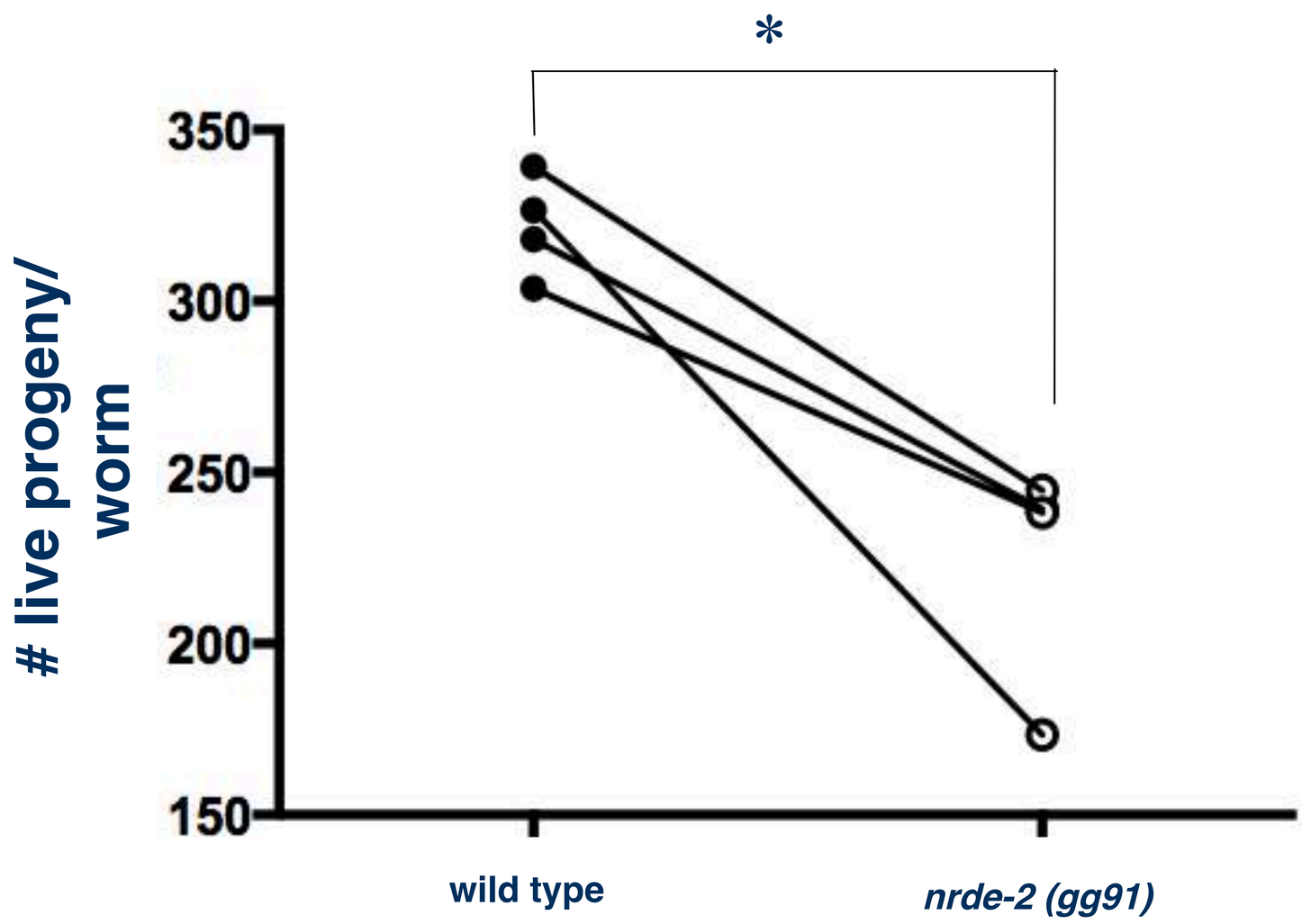

Figure S1: Loss of NRDE-2 significantly decreases brood size as compared to wild type worms when propagated at 20°C. Each data point represents one biological replicate of 16 worms per experiment (n=4; *p=0.0148, paired Student's t test).

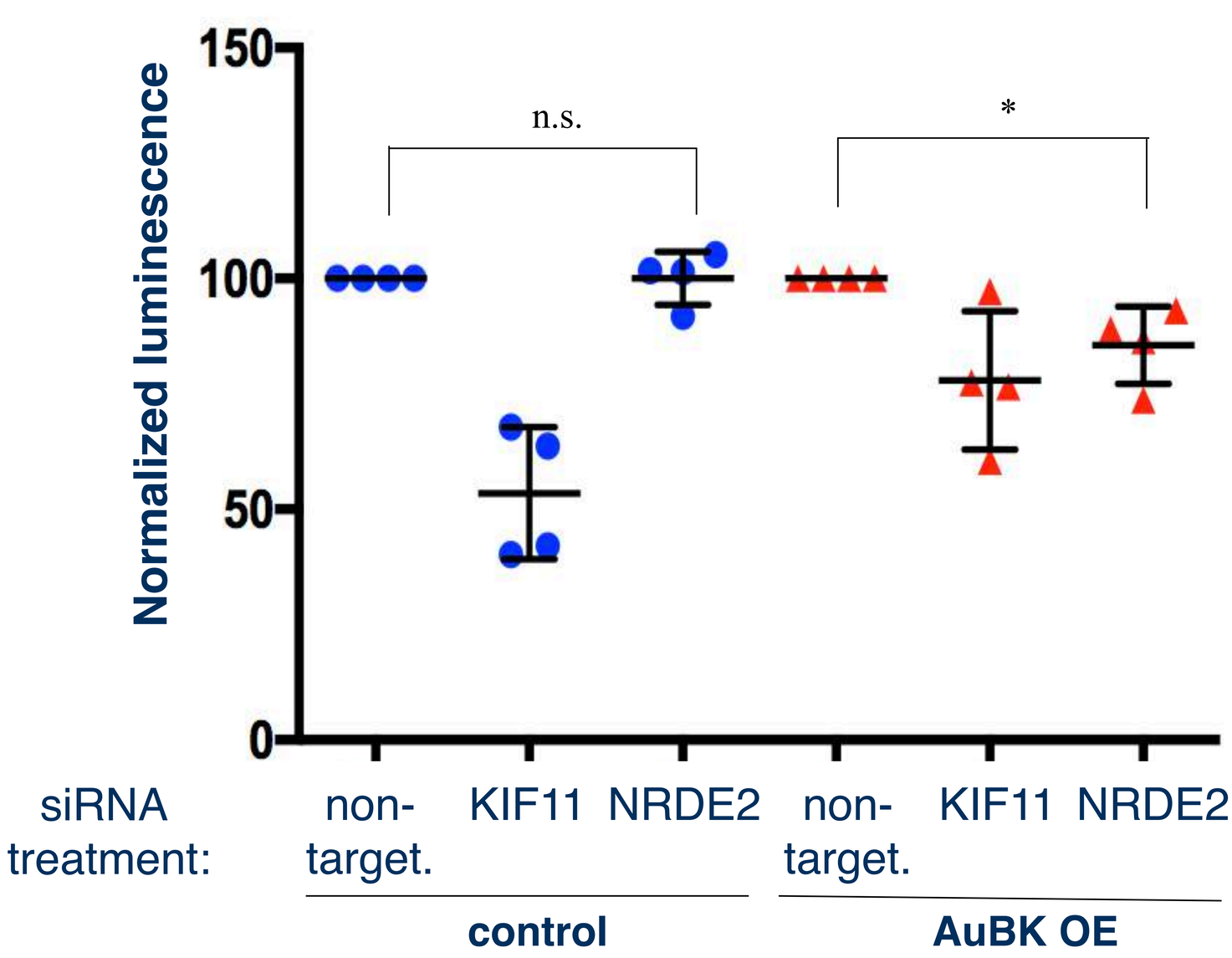

Figure S2: NRDE2 knockdown decreases cell viability in AuBK OE cells but not in control cells. The Cell Titer Glo assay measures the number of metabolically active cells by quantifying the amount of ATP present in the cell culture. The luminescent signal was normalized to non-targeting siRNA treated cells in both control cells and AuBK OE cells. KIF11 siRNA was used as a positive control. Control cells treated with NRDE2 siRNA (100.0 ± 2.890, n=4) had no change in luminescence as compared to control cells treated with non-targeting siRNA. AuBK OE cells treated with NRDE2 siRNA (85.55 ± 4.167, n=4) had a lower amount of luminescence as compared to AuBK OE cells treated with non-targeting siRNA (*p=0.0133). P-values determined using unpaired Student's t test.

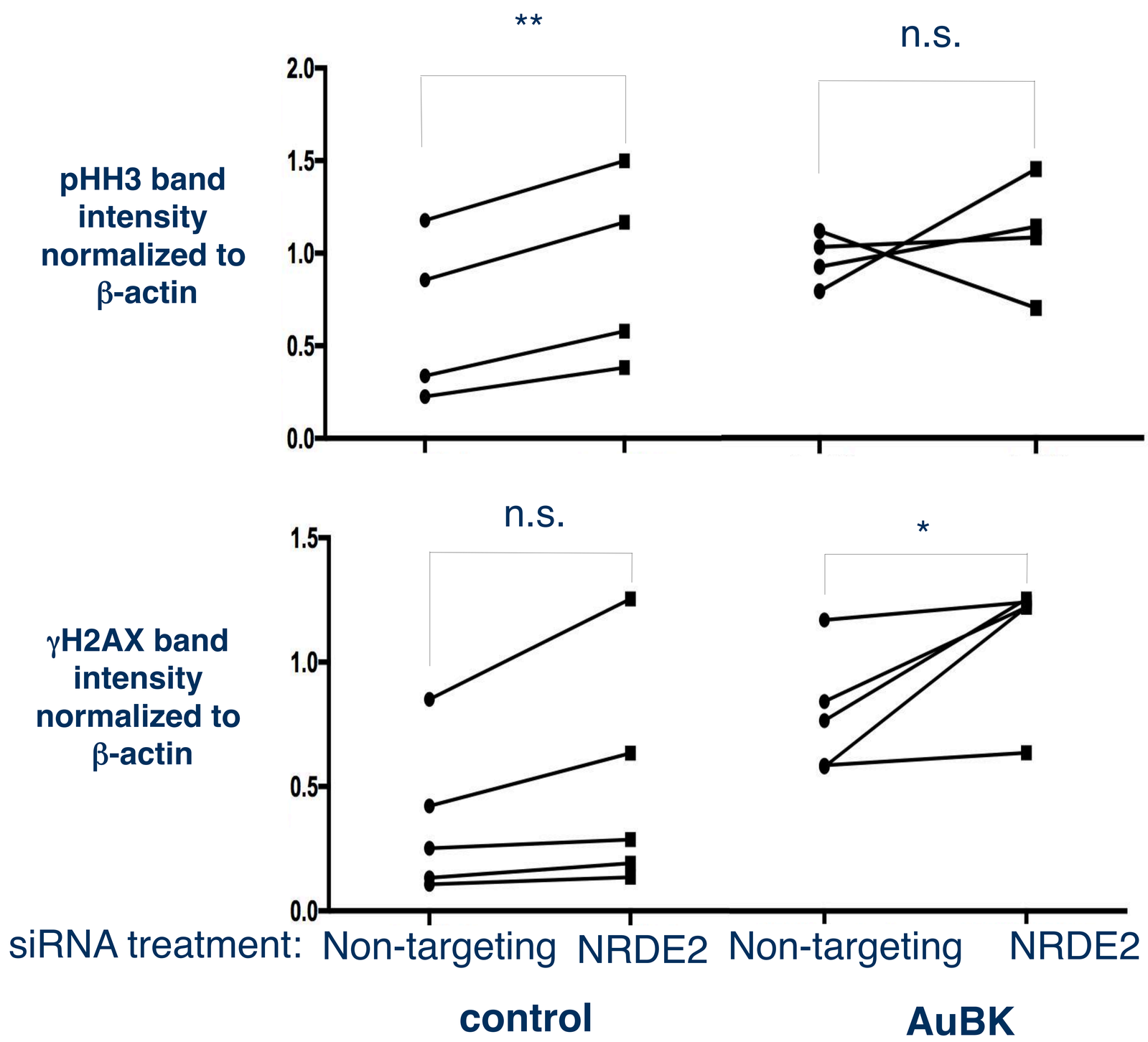

Figure S3 (Top) Loss of NRDE2 in control cells increases pHH3 levels as compared to control cells treated with non-targeting siRNA (n=4, p=0.0068). In contrast, loss of NRDE2 in AuBK OE cells does not change pHH3 levels (p=???). (Bottom) Loss of NRDE2 in control cells does not alter levels of γH2AX (p=????), however in AuBK OE cells, loss of NRDE2 increases γH2AX levels. (n=5, *p= 0.0483) All p-values determined using paired student's t test.

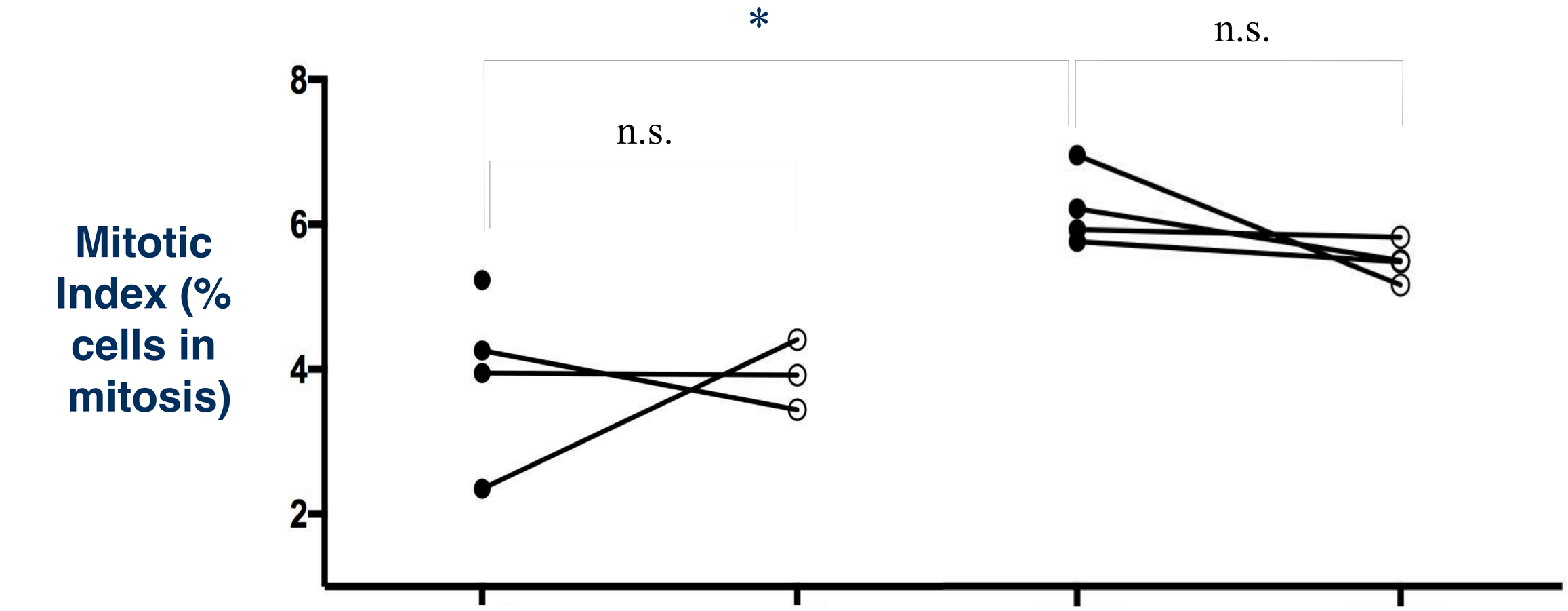

Figure S4: Loss of NRDE2 in MCF10A cells does not significantly change the mitotic index. Mitotic Index calculated by dividing total number of cells in mitosis by total number of cells in the population. AuBK overexpressing cells have a significantly higher basal mitotic index than control cells (*p= 0.0315, student's paired t test).

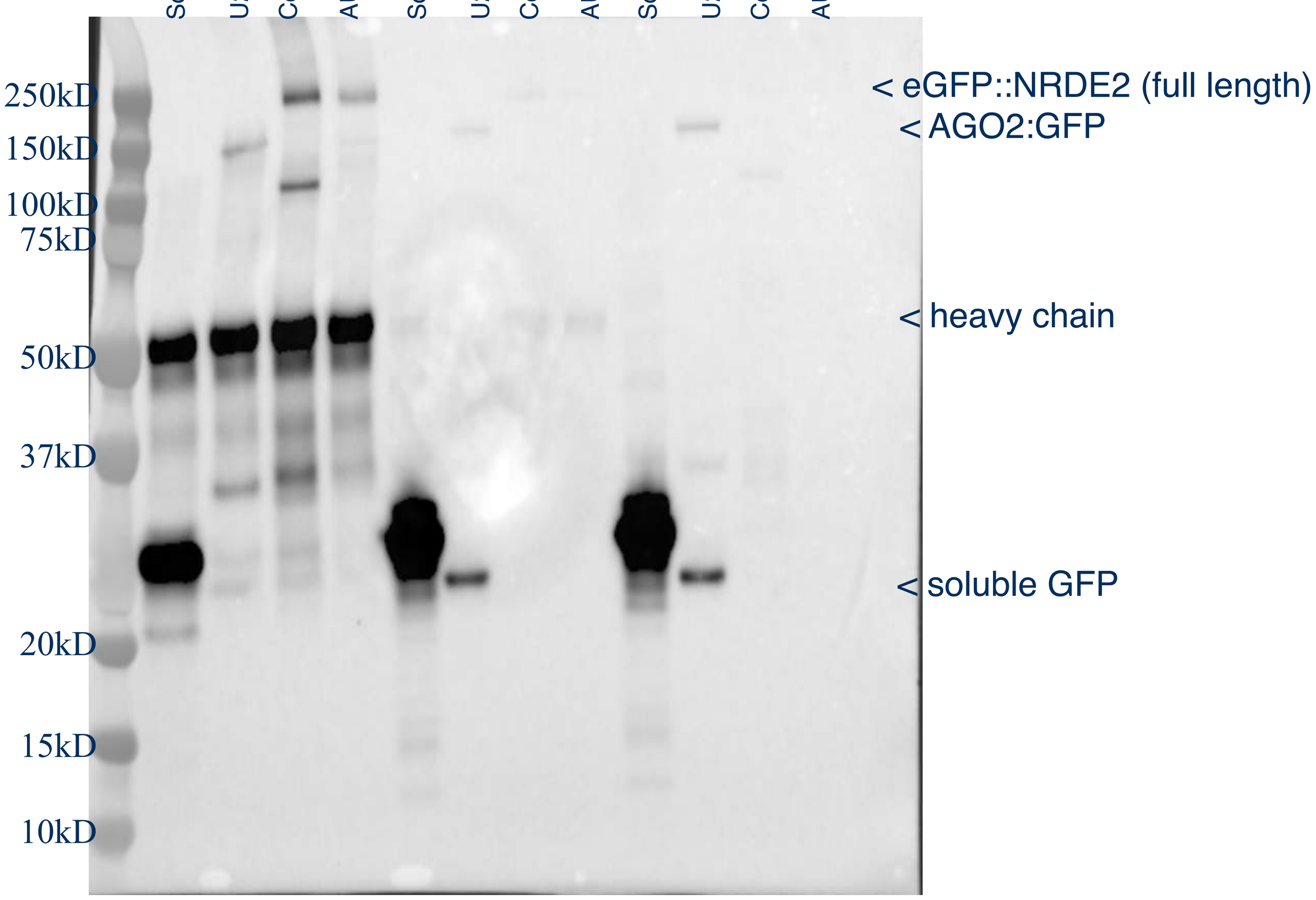

Figure S5: Representative western blot of MCF10A cell lysates. Co-IP was performed using goat Anti-GFP antibody to pull down eGFP::NRDE2 from MCF10A cell lysates. Western blots were developed using rabbit anti-GFP polyclonal antibody to detect eGFP::NRDE2 and soluble GFP.

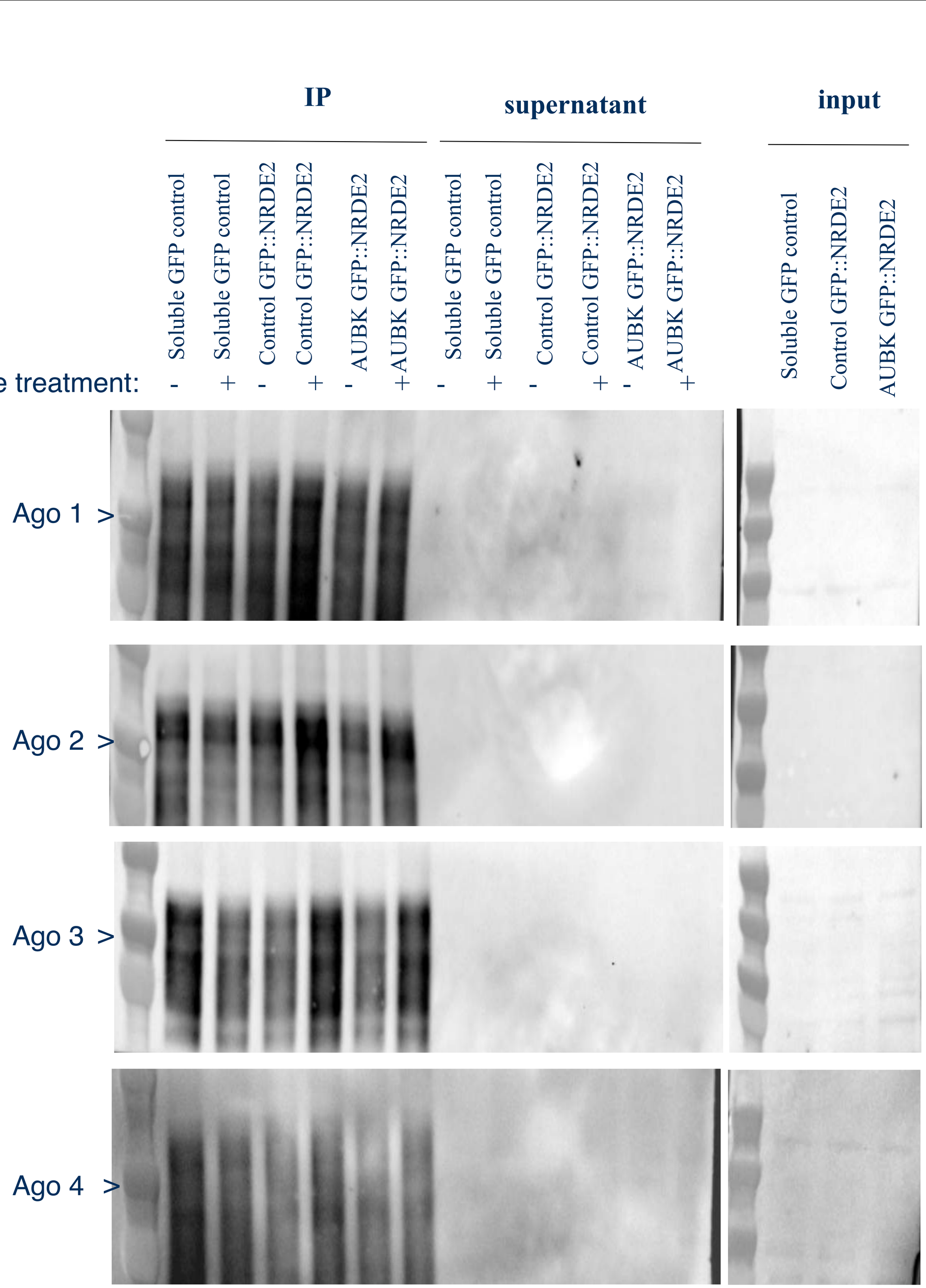

Figure S6: NRDE-2 does not interact with the mammlian argonautes Ago 1,2,3 or 4. Goat anti-GFP used to pull down eGFP::NRDE2 in MCF10A lysates in co-IP assay. Western blots against human Ago1-4 show no interaction with eGFP::NRDE2. Arrows point to 97kD, the expected size of each Ago protein.

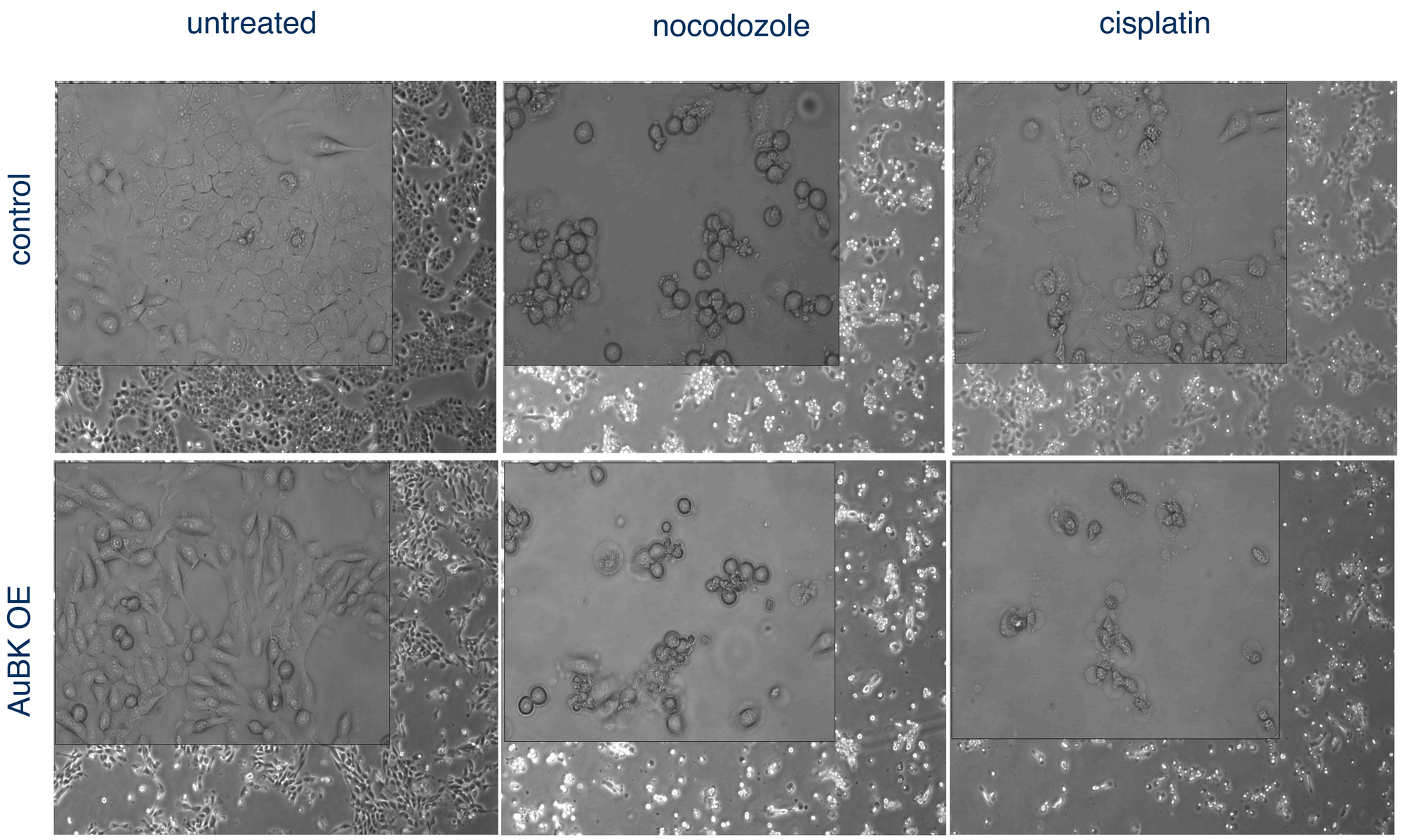

Figure S7: Control and AuBK OE MCF10A cells treated with nocodozole show rounded morphology consistant with stall in G2/M. Cells treated with cisplatin show rounded, fragmented morphology, consistant with apoptosis.
Representative brightfield images of cells taken 16 hours after 0.1ug/ml nocodozole or 60uM cisplatin drug treatment with 4x objective and 20x objective (inset).